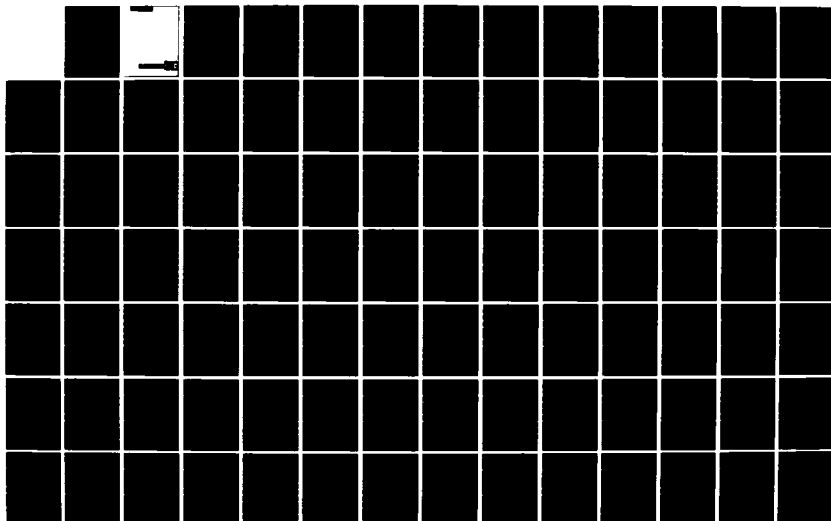AD-A131 388　　SEDIMENT TRANSPORT IN A TIDAL INLET(U) WOODS HOLE　　1/2
　　　　　　　　OCEANOGRAPHIC INSTITUTION MA　D G AUBREY ET AL. JUN 83
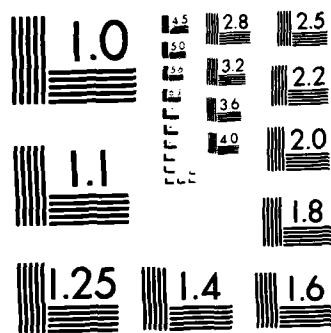　　　　　　　　WHOI-83-20 ARO-16710.8-GS DAAG29-81-K-0004
UNCLASSIFIED　　　　　　　　　　　　　　　　　　　F/G 8/3　　　　NL

MICROCOPY RESOLUTION TEST CHART

NATIONAL BUREAU OF STANDARDS 1963-A

To examine this problem, we have restricted the study to relatively
shallow bays (water depths of same order as tidal range) with negligible fresh
water inflow. Consequently the estuarine channels are well-mixed, and we can
ignore buoyancy effects in the models. As described in the following section,
our approach has been to combine diagnostic numerical modeling with careful
field experimentation to assure a field-tested predictive tool for non-linear
tidal distortion. Field work for this program covered the two experiments
from 1981 and 1982 (NI81 and NI82), discussed previously.

## Introduction

The character of the offshore tide is strongly modified in its propagation
through the shallow inlet/estuarine systems of interest. Time asymmetries

WHOI-83-20

# SEDIMENT TRANSPORT IN A TIDAL INLET

by

David G. Aubrey and Paul E. Speer

**WOODS HOLE OCEANOGRAPHIC INSTITUTION**
Woods Hole, Massachusetts   02543

June 1983

## TECH.·ICAL REPORT

**Approved for Distribution:** _R. P. Von Herzen_

Richard P. von Herzen, Chairman
Department of Geology and Geophysics

## FOREWORD

# TABLE OF CONTENTS

FIGURES

## TABLES

## STATEMENT OF PROBLEM

Research performed over the duration of the contract was centered on clarifying different aspects of sediment transport around natural, unstructured tidal inlets subjected to both wave and tide forcing. The research proposal specified seven general questions to be addressed as part of the Nauset Inlet study; all have been examined as part of this research. Rather than follow the outline of the proposed work, results of our research are more logically presented in the following order:

1). Diagnostic numerical modeling of the non-linear growth of tidal disturbances in shallow estuarine systems, and its implications for sediment transport (hence long-term fate of estuarine systems);

2). Effects of flow curvature on spatial non-homogeneity of tidal inlet flows, and resultant sediment transport;

3). Clarification of mechanisms for updrift migration of natural, unstructured tidal inlets;

4). Hypothesis of mechanisms by which barrier beaches can rapidly elongate under conditions of minimal net longshore sand transport;

5). Description and quantification of sea-level rise throughout the United States coastlines over the past century;

6). Historical description of tidal inlet and barrier beach behavior over the past three centuries as corroborative data for evaluating the generality of our inlet sediment transport modeling studies;

7). Miscellaneous technical details related to the conduct of nearshore research were published, including studies of low-cost cable joining in near-shore environments; description and intercomparison of instrumentation and analysis routines for estimating directional spectral parameters from wave gage data; and the development of an automated system for acquiring precise nearshore bathymetric data, including data acquisition, processing, and plotting of tides, bathymetry and navigation.

The study of tidal inlets and estuaries has application to a diverse spectrum of concerns. A primary task of the U.S. Army Corps of Engineers is to assure navigability of inland waters, and tidal channels leading into those inland waters. Inlet behavior and flushing are primary considerations for those interested in coastal water quality, and its associated pollution implications. Shell and fin fisheries are sensitive to changes in water quality and tidal exchange, so changes in inlet configuration can affect the viability of these animals, as well as the plant life sustaining them. The U.S. East and Gulf coasts are particularly sensitive to inlet and bay processes, since these represent the longest stretch of barrier beaches and tidal inlets in the world. In all, barrier beaches and their associated tidal inlets cover approximately 13°/° of the world's coastline (King, 1972), most occurring in areas with low to moderate tidal range.

## RESULTS

Seven major elements of the tidal inlet study listed in the previous section are discussed in detail over the following pages. Where papers or scientific talks have been prepared for a particular topic, abstracts from these are inserted into the text with appropriate references, to reduce the length of the report. For unpublished work, a more lengthy discussion of the work is presented.

Field work for this study was undertaken over two summers (1981 and 1982). Field work particularly emphasized elements 1, 2, and 3 of the work statement. During 1981, a two-week intensive field program was held from 12-27 September at Nauset Inlet, Cape Cod, Massachusetts (figure 1 and 2). Work during this period emphasized measurement of currents near the inlet channel, measurement
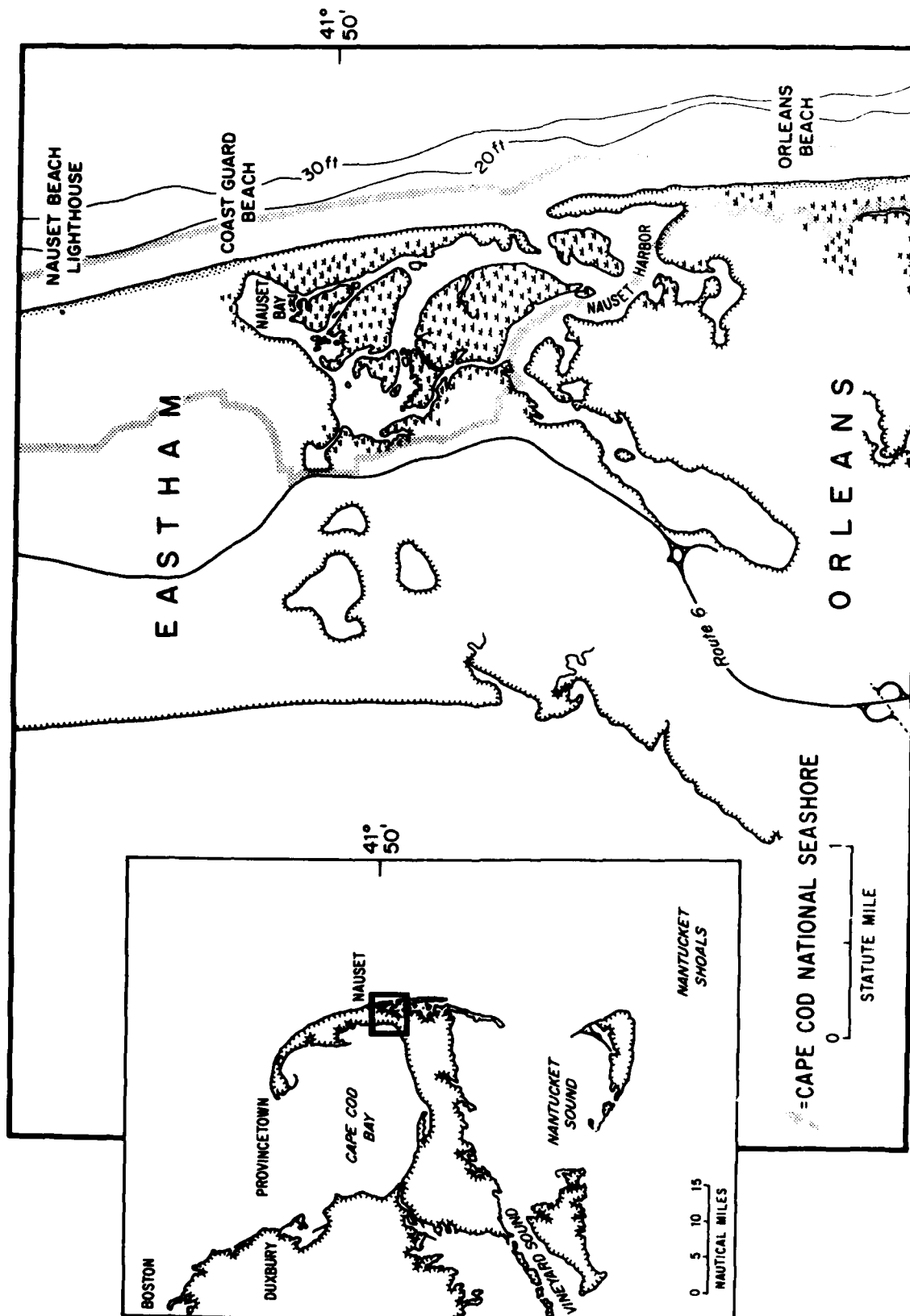
Figure 1. General location map for Nauset Inlet, Cape Cod, Massachusetts.

NAUSET INLET
LOW TIDE
21 SEPTEMBER 1981
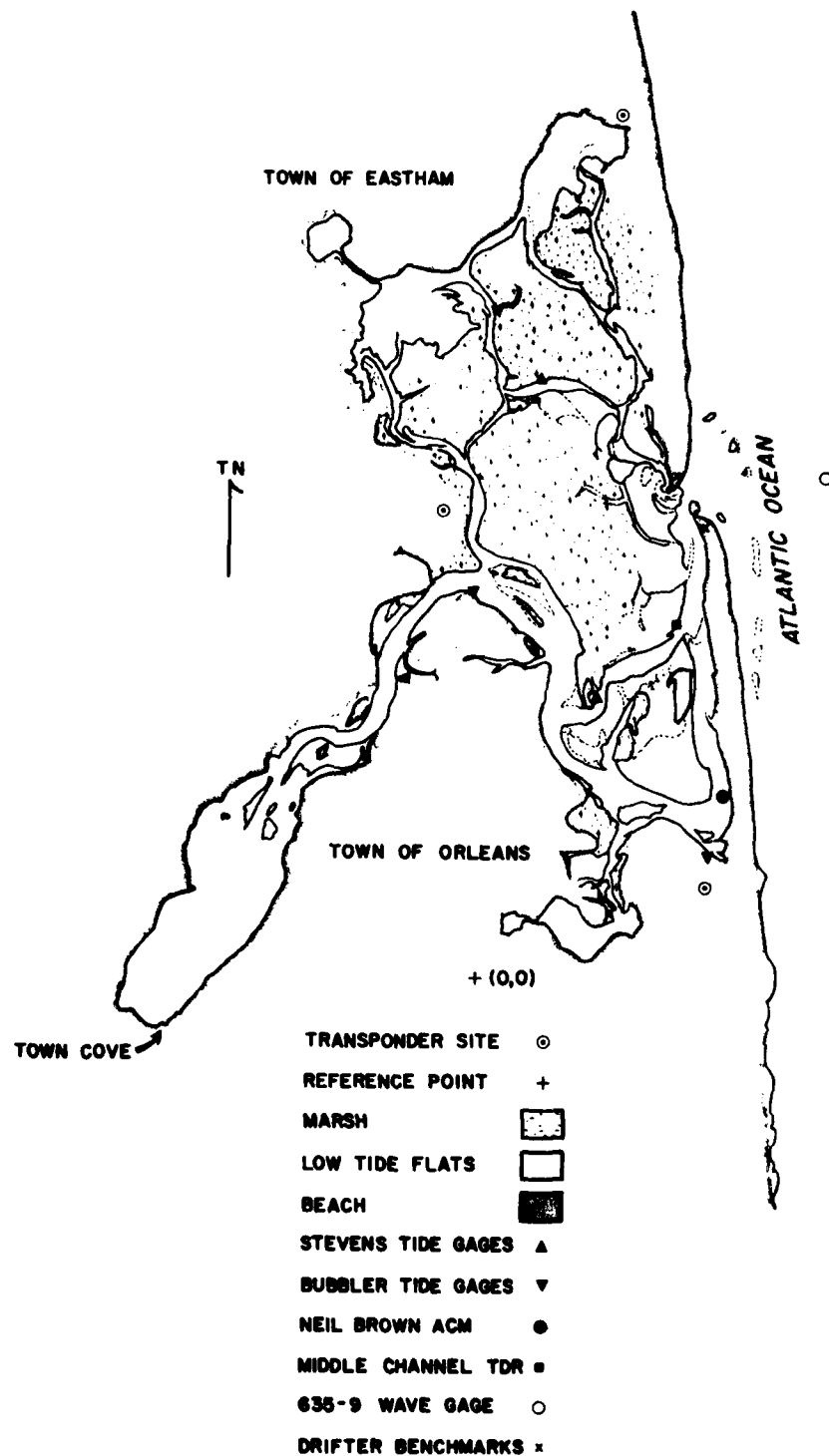
Figure 2. Instrument locations for Nauset Inlet experiment of September, 1981, shown on a base map depicting limits of low tide exposure taken from a vertical aerial photograph of the study area during the experiment. North Channel tide ga... at uppermost triangle in the figure.

of tidal elevation throughout the estuary, drogue tracking on flood and ebb flow, and measurement of sea surface gradients through the inlet proper. Instrument locations are in Figure 2 and described in Table 1. Specific elements of the experiment will be discussed in more detail below. This experiment will be referred to as N.I.81.

The second field experiment (N.I.82) took place from 21 August to 5 September 1982, again at Nauset Inlet (figure 3). This experiment emphasized wave measurements, current and sea surface measurements to estimate local stress balances, bedform migration studies and detailed tidal measurements over three months to clearly document the phase and amplitude characteristics of the tidal disturbance propagation through a shallow estuary. The field experimentation plan is contained as Table 2 and Figure 3. Specific aspects of this experiment will be discussed in the following detail of individual work elements.

TASK    1). <u>Non-linear growth of tidal distortion in shallow estuarine systems</u>: Because sediment transport in and around tidal inlets depends not only on conditions seaward of the inlet, but also landward, we have spent some effort modeling the distortion of the astronomical tide within the bay/estuary served by the tidal inlet. Tidal distortion caused by bay geometry affects tidal flows near the inlet mouth, thus affecting patterns of sediment transport. The long term fate of estuaries is partly a function of net import or export of sediment in an inlet/bay system. As an example, when flood tide duration exceeds ebb tide duration, maximum flow velocities will occur during ebb (preserving continuity), thus enhancing ebb sediment transport since the transport function is highly non-linear in velocity. Conversely, when ebb duration exceeds flood, maximum flow velocities will occur during flood, thus enhancing sediment transport during flood.

TABLE 1

| TASK | INSTRUMENTATION |
|------|-----------------|
| Current profiling | Benthic Acoustic Stress Sensor (BASS)<br>MM 511 current meter<br>Neil Brown Acoustic Current Meter |
| Bedform monitoring | Bedform monitor (Williams and Grant)<br>Repeated echo-sounder profiles |
| Tide gaging | Stevens Tide Gages (2)<br>Bubbler Tide Gages (2)<br>Sea Data TDR-1A's (5) |
| Directional wave gaging | Sea Data 635-9 directional wave gage |
| Lagrangian flow field | Surface drifters (21 on ebb tides,<br>13 on flood tides) |
| Land surveys | Conventional rod and engineer's level. |
| Water surveys | Navigation: Del Norte Trisponder<br>Bathymetry: Raytheon DE719C |

Summary of equipment and major tasks during the Nauset Inlet 1981 experiment.
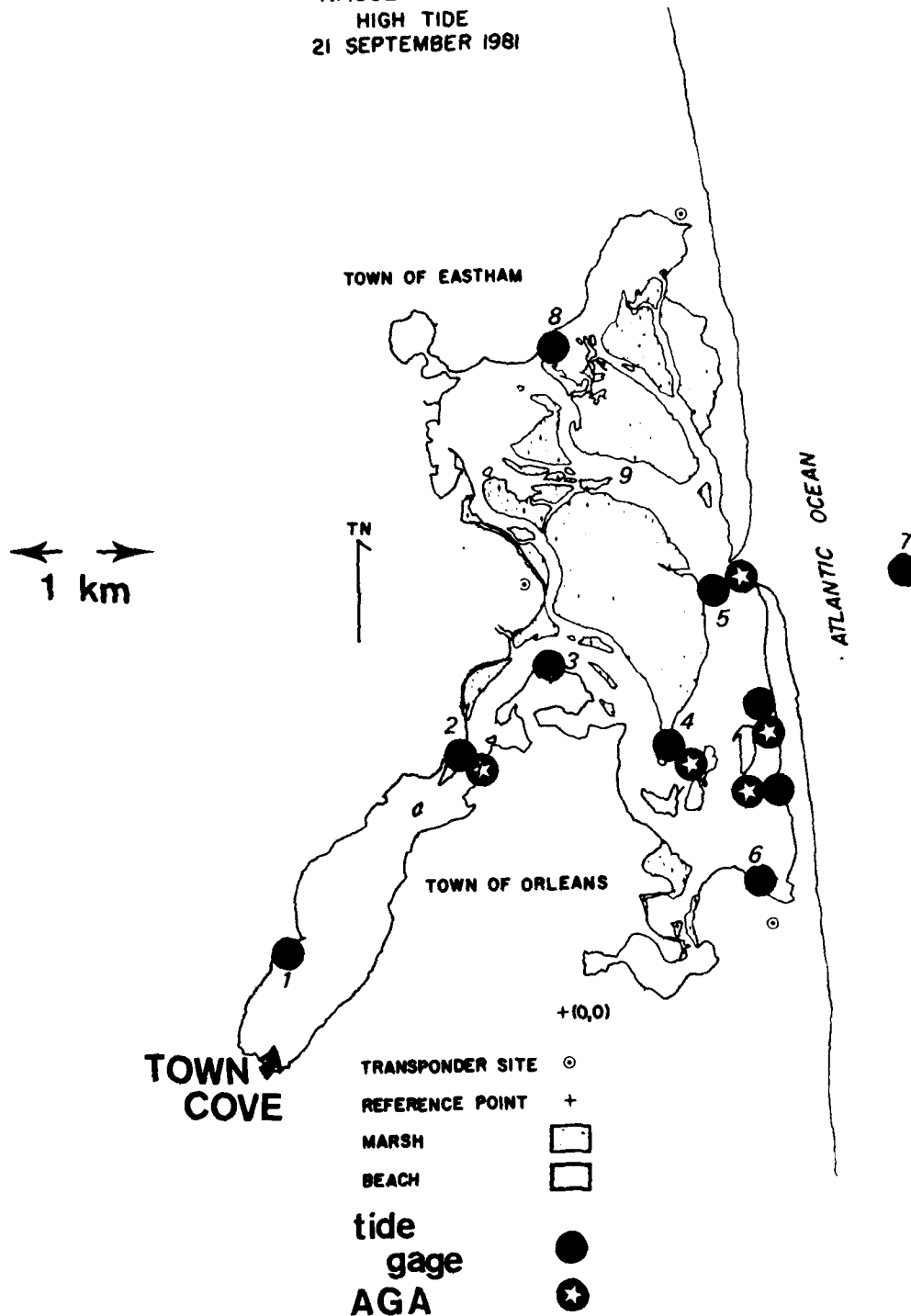
Figure 3. Location map for Nauset Inlet experiment of August through October 1982. Numbers refer to locations referenced in the text and other figures: 1-Goose Hummock, 2-Mead's Pier, 3-Snow Point, 4-Middle Channel West, 5-Middle Channel East, 6-Nauset Heights, 7-Ocean wave and tide gage, 8-Nauset Bay. Base map was compiled from topography of 1981, referenced to high tide levels showing primary tidal channels more clearly.

TABLE 2

| TASK | INSTRUMENTATION |
|------|-----------------|
| Current profiling | AGA current meter system (5 element electromagnetic current sensing system) Neil Brown Acoustic Current Meter |
| Bedform monitoring | Repeated echo-sounder profiles |
| Tide gaging | Steven's model 71-A tide gages (2) Steven's model 7030 tide gages (12) Sea Data TDR-1A (3) |
| Directional wave sensing | Sea Data 635-9 directional wave gage |
| Land surveys | Conventional rod and engineer's level |
| Ocean surveys | Navigation: Del Norte Trisponder system Bathymetry: Raytheon DE719C with digitizer. |
| Offshore currents | VMCM array in 50 m water depth (3) |
| Cross-channel and down-channel gradients | Sea Data TDR-1A (3) |

Summary of equipment and major tasks during the Nauset Inlet 1982 experiment.

To examine this problem, we have restricted the study to relatively shallow bays (water depths of same order as tidal range) with negligible fresh water inflow. Consequently the estuarine channels are well-mixed, and we can ignore buoyancy effects in the models. As described in the following section, our approach has been to combine diagnostic numerical modeling with careful field experimentation to assure a field-tested predictive tool for non-linear tidal distortion. Field work for this program covered the two experiments from 1981 and 1982 (NI81 and NI82), discussed previously.

## Introduction

The character of the offshore tide is strongly modified in its propagation through the shallow inlet/estuarine systems of interest. Time asymmetries develop, resulting in a distorted tide with unequal rise and fall. This time asymmetry in the vertical tide, in turn, leads to asymmetries in the magnitude of ebb and flood velocities within tidal channels (e.g., Boon and Byrne, 1981). Depending on the physical characteristics of the particular inlet and estuary, the tide may be strongly damped, or in cases amplified (e.g., Byrne et al., 1977; Aubrey and Speer, 1982). The modified tide interacts with the estuary to strongly influence patterns of net sediment transport. Over short time scales, the interaction has important implications for channel navigability. On long (geologic) time scales, the implications are for estuary infilling or stability. The geologic development of an inlet/estuarine system will alter its hydrodynamic response; consequently during its development an inlet/estuarine system may change from flood-domination to ebb-domination (or vice versa). This hydrodynamic variation may profoundly influence geological history of these coastal environments.

Tidal distortion is represented by non-linear growth of harmonics of the principal diurnal and semi-diurnal components of the offshore tides, as well as interactions among these components. In areas dominated by semi-diurnal tides, the hypothesis is that the distortion is caused principally by harmonics of the $M_2$ (lunar semi-diurnal) component (e.g., Pingree and Griffiths, 1979; Uncles, 1981; Boon and Byrne, 1981). Both dynamic and kinematic effects are responsible for the non-linear harmonic growth. Each inlet/estuarine system has a particular set of physical characteristics (channel/basin geometry and friction) which interact with the tide to produce the harmonic growth. Consequently, growth rates and phase relationships differ from one estuary to the next. Of particular interest are systems with exceptionally strong harmonic growth leading to dramatic tidal asymmetries (e.g., Nauset Inlet, Aubrey and Speer, in prep.). Such systems in some way may be "tuned" such that harmonic growth is vigorous. The importance of the various mechanisms producing the harmonic growth needs to be assessed to understand how these systems respond to tidal forcing. This information can then yield insight into both the short- and long-term fate of an estuary through consideration of resulting net sediment transport patterns.

Non-linear terms are also responsible for generating residual (i.e., tidally averaged) flows. An estuary which responds to tidal forcing in a strongly non-linear fashion may also develop significant residual flows. These residual flows can play an important role with respect to flushing times of estuaries. Therefore, non-linear tidal response of estuaries is important not only for sediment transport patterns but also for dispersal of water column contaminants. Residence times of these contaminants (either particulate or dissolved) can be assessed with the ensuing modeling.

-15-

## Discussion of Physical Problem

Harmonics (or overtides) of the principal tidal constituents are generated by non-linear terms in the equations of motion. Principal overtides of interest are the $M_4$, $M_6$ and $M_8$ constituents, which are the second, third, and fourth harmonics of $M_2$. The physical problem considered here is the generation of harmonics in basins co-oscillated by tidal forcing through an inlet. As mentioned previously, we are considering systems small enough to neglect Coriolis accelerations, and well-mixed so that their dynamics may be adequately treated by depth-integrated models. Three sources of non-linearities are identified by consideration of the simplified one-dimensional equations of motion for a tidal channel (e.g., Dronkers, 1964; analogous terms are found in the 2-D equations, see Appendix I):

$$\frac{\partial \zeta}{\partial t} + \underbrace{\frac{1}{b}\frac{\partial}{\partial x} A \cdot \bar{u}}_{I} = 0 \qquad \text{Continuity}$$

$$\frac{\partial \bar{u}}{\partial t} + \underbrace{\frac{\partial \bar{u}^2}{\partial x}}_{II} = \frac{-g\partial \zeta}{\partial x} - \underbrace{\frac{C_D |\bar{u}|\bar{u}}{(h+\zeta)}}_{III} \qquad \text{Momentum}$$

where

$\bar{u} = \frac{1}{A}\int u\, dA$ = average down channel velocity

$h$ = undisturbed water depth

$\zeta$ = tidal elevation perturbation

$A$ = cross-sectional area, which is a function of tidal stage

$b$ = channel width, which can be a function of tidal stage

$C_D$ = drag coefficient

$x$ = coordinate directed along axis of channel

Underlined terms designated by Roman numerals which are responsible for generating harmonics can be described as follows:

I) interactions between the tidal current and changes in cross-sectional area.

II) advection of momentum

III) quadratic friction: Friction is an inherently non-linear process typically parameterized in a quadratic form in depth-averaged models. If $M_2$ is the principal tidal component, note that a quadratic friction will spread energy into odd harmonics.

if $\tau_b = \rho C_D |\bar{u}| \bar{u}$     with $u = u_0 \cos\omega t$

then

$$\tau_b = \frac{8}{3\pi} \rho C_D u_0^2 (\cos\omega t + \frac{1}{5} \cos 3\omega t ...)$$

However, the friction term in the one-dimensional momentum equation is divided by $(h + \zeta)$, producing even harmonics.

The importance of these terms will differ from one estuary to the next, according to the dominant physical scaling. They will all combine to produce tidal distortion of different magnitudes and types (e.g., flood or ebb asymmetry). The physical picture is complicated by several factors. The most important is the presence of many components in the offshore tides with possible interactions among them and their harmonics within the estuary, complicating dynamic interpretations. However, in areas where one component is dominant ($M_2$ in most of our cases of interest), the principal contributions to tidal asymmetry will be harmonics of that component.

For the sake of completeness, we also note that steady (i.e., residual) terms result from the non-linear terms in the form of a Lagrangian mean velocity (e.g., Longuet-Higgins, 1969; Van de Kreeke, 1976; Van de Kreeke and Chiu, 1980). This mean velocity is important if one considers the flushing time of tidal channels (see Appendix I), or sediment transport.

## Previous Work

A large amount of work has been performed on tidal inlets and their associated estuaries; however, none of it specifically addresses the problem outlined in the introduction. The background work of interest centers on analytical and numerical modeling (plus geologic interpretations) performed on tidal channels and inlet/estuarine systems. The U.S. Army Corps of Engineers funded a program of study on several inlets through the General Investigation of Tidal Inlets (GITI) program. These studies included kinematic measurements at several inlets and a numerical modeling program. Included in this work are examples of tidal asymmetries (e.g., Watson and Behrens, 1976; Finley, 1976; Nummedal and Humphries, 1978) but no attempts to assess generating mechanisms quantitatively. A number of numerical models were developed to investigate inlet hydraulics (e.g., Seelig et al., 1977; Masch et al., 1977; Chen and Hembree, 1977). These models, particularly the two-dimensional models, are essentially predictive. They are forced with boundary conditions and tuned frictionally to reproduce observed conditions (both field and laboratory) as closely as possible. They were not presented as diagnostic tools for investigating problems such as non-linear generation of tidal harmonics. While these models suggest the possibility of predicting inlet hydraulics to a reasonable degree (excepting, of course, sediment transport), they do not shed light on the hydrodynamic problem of interest: What characteristics of inlet/ estuarine systems cause them to develop different patterns and rates of growth of tidal asymmetries  Seelig and Sorensen (1978) used the numerical model of Seelig et al. (1977) to examine the effect of certain physical parameters (e.g., changing basin area with tidal stage, tide/storm surge interaction) on estuarine tidal response. However, they did not examine the hydrodynamic

source of non-linearities. None of these papers include spectral comparisons of model results to data. This spectral approach is essential if one is to quantitatively understand the tidal response of these systems, and correctly define the sources of non-linearities.

Many analytical models (both linear, such as LeBlond, 1978, and Robinson, 1980; and non-linear, such as Kreiss, 1957, Dronkers, 1964, Ianniello, 1977, and Uncles, 1981) have been developed to examine aspects of tidal propagation in channels or rivers, including the problem of tidal distortion. Kreiss (1957) noted the frequent occurrence of tidal current time and velocity asymmetries in estuaries. The case he studied had flood currents which were shorter in duration but reaching greater peak velocity than ebb. He explained this behavior as a result of advective non-linearities and frictional effects. This model, like most others, requires $\zeta/h \ll 1$, and in addition is strictly valid for relatively weak friction. Ianniello (1977) examined another aspect of the non-linear behavior of tides in a channel: tidally-induced residual currents. His model also requires $\zeta/h \ll 1$. Van de Kreeke and co-workers (1975, 1976, 1977) examined residual flows in tidal channels as an indicator of flushing or renewal times. All three models (Kreiss, Ianniello and Van de Kreeke) employ simple geometry. Dronkers (1964) developed a quasi-numerical model which can reproduce tidal asymmetry. It imposes implicit restrictions on tidal amplitude ($\zeta/h \ll 1$). LeBlond (1978) studied the case of tidal propagation in the presence of strong friction (and with freshwater inflow). He presented a model which explains tidal propagation in this environment as an essentially diffusive process. Although these models all provide insight to the problem of tidal propagation, they do not address complicated bathymetry (where time-varying geometry is likely an important source of non-linearities).

Additionally, they are all limited to the weakly non-linear case of $\zeta/h \ll 1$, whereas some inlet/estuarine systems are strongly non-linear in this coefficient (e.g., Nauset Inlet, MA, Aubrey and Speer, 1982).

A number of non-linear numerical model investigations of tidal behavior in shallow seas and rivers exists (Pingree and Maddock, 1978; Pingree and Griffiths, 1979; Uncles and Jordan, 1980; Uncles, 1981). Pingree and Maddock (1978) and Uncles (1981) in particular focus on generation of the $M_4$ and $M_6$ tidal components and attempt to assess the dominant mechanisms. Pingree and Maddock (1978) modeled the English Channel, a region with substantially different physical characteristics than the systems considered in this proposal (e.g., small tidal amplitude/mean depth ratio, large horizontal scales, important Coriolis effects). Pingree and Griffiths (1979) extended this work to look at sediment transport paths resulting from the non-linear tidal distortion. Uncles (1981) considered the problem of residual current generation. He did not specifically deal with tidal asymmetries which are central to the problem of sediment transport. These studies concentrated on large systems, so data comparisons were relatively sparse.

Boon and Byrne (1981) performed some numerical modeling to investigate asymmetries in tidal inlets and attempted to link their findings to the eventual fate of estuarine systems. They do not focus on the specific hydrodynamic mechanisms by which harmonics are generated. Also there is insufficient quantitative comparison with field data to evaluate mechanisms and rates of harmonic growth. Clearly, there has existed a need for careful numerical modeling coupled with well-designed field experiments to examine the problem of tidal propagation within inlet/estuarine systems. Numerical modeling is required because the bathymetry of such systems is frequently complex and, in cases, they may be highly non-linear. The data is required in order to allow quantitative spectral comparisons with model results.

## Field Work--Nauset Inlet, Cape Cod, MA

For the past two years, we have been examining the problem of tidal distortion in a shallow inlet/estuarine system, Nauset Inlet, MA (figure 1). The study has involved both an extensive field effort designed to quantify the tidal asymmetry in this estuary, as well as a numerical modeling program to investigate the generation mechanisms. The offshore tide is predominantly semi-diurnal with a range of two meters (figure 4). Nauset is a shallow system (4-5 m inlet channel, 2-3 m deep southern channels, <1 m deep northern channels) terminating to the south in a 5-6 m deep body of water, Town Cove. Based on field measurements, Nauset may be characterized as a strongly non-linear, frictionally-dominated system. The $M_4$ tidal component grows dramatically as the tide propagates through the estuary (figure 5 and 6). The result of this harmonic growth is a strong time asymmetry, with falling tide exceeding rising tide by 1 to 4 hours, increasing with distance into the estuary (Table 3 and figure 7). This should be contrasted with other inlet/estuaries displaying a time asymmetry favoring flood and much weaker harmonic growth (e.g., Wachapreague Inlet, VA, Byrne et al., 1977; Ocean City Inlet, MD, Boon and Byrne, 1981; North Inlet, SC, Nummedal and Humphries, 1978). Nauset's strong asymmetry in the surface tide affects currents in the inlet throat and other estuarine channels. A velocity record from a tidal channel at Nauset (figure 8) graphically illustrates the extremely distorted tide. Clearly, at this location, sediment transport will be enhanced during the flood cycle (with important implications for estuary infilling). The tide is strongly attenuated at Nauset with the tidal range decreasing by 30°/∘ to the south (3 km from the inlet) and 50°/∘ to the north (1.5 km from the inlet).

# NAUSET INLET TIDES
## OCEAN TIDE GAGE
## 10/82–11/82

M4/M2 = 0.0049

M6/M2 = 0.0039
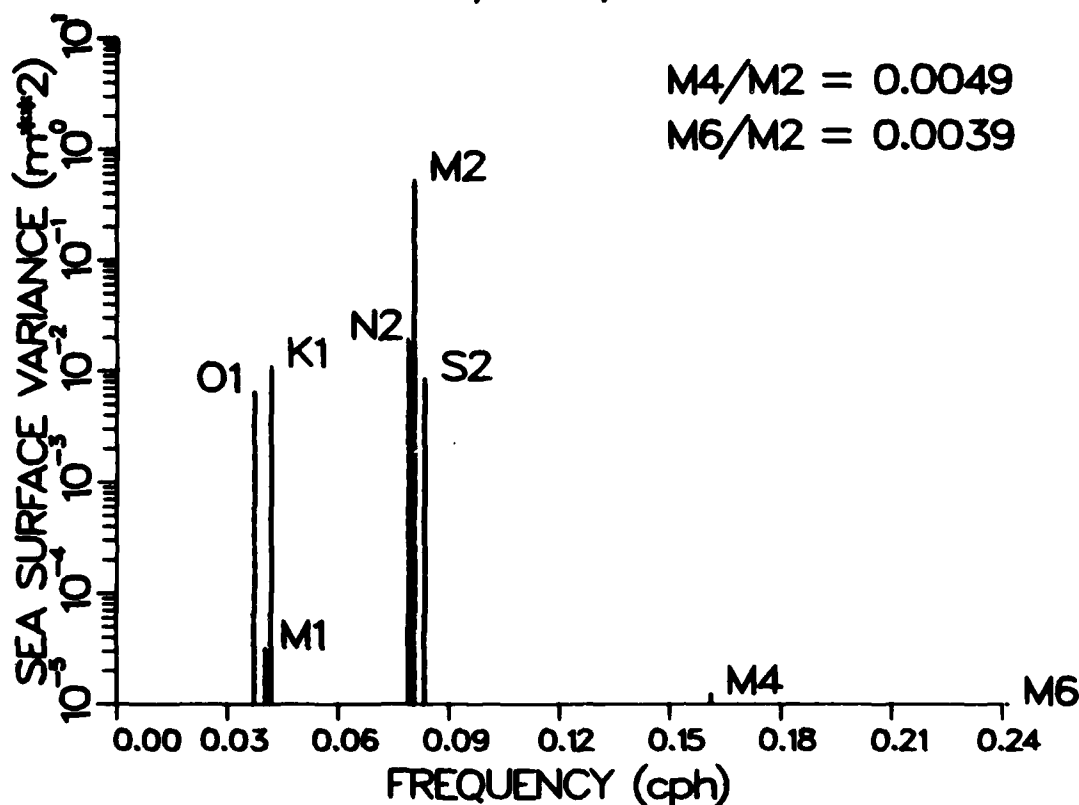


Figure 4. Periodogram derived from tidal harmonic analysis of pressure sensor data located in 10 m water depth outside the inlet (location 7 in figure 3). Subscripted letters refer to tidal constituents with $M_2$ (the principal lunar semidiurnal tide) the dominant constituent. Tidal harmonics of the $M_2$ tide are shown as $M_4$ and $M_6$ (the overtides). Relative size of the ratios $M_4/M_2$ and $M_6/M_2$ specifies the degree of non-linearity of the tides. In this case the ratios are low, so the tide is weakly non-linear. Ratios indicated are for amplitudes, not energy.

NAUSET INLET TIDES
MIDDLE CHANNEL WEST TIDE GAGE
10/82–11/82
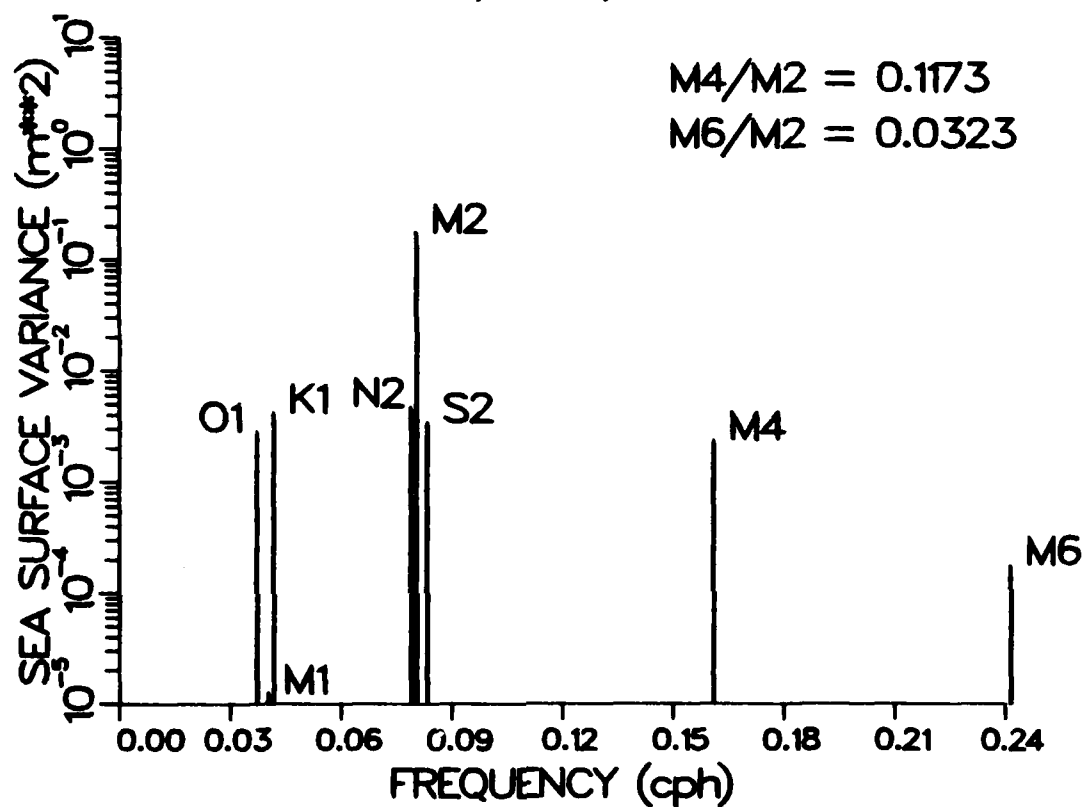
**Figure 5.** Periodogram of tides within the estuary (location 4 in figure 3). The non-linear ratios $M_4/M_2$ and $M_6/M_2$ are much larger than in figure 4, showing the growth of the non-linearities from deep to shallow water.

**NAUSET INLET TIDES**
NAUSET BAY TIDE GAGE
10/82–11/82

M4/M2 = 0.2659
M6/M2 = 0.0415
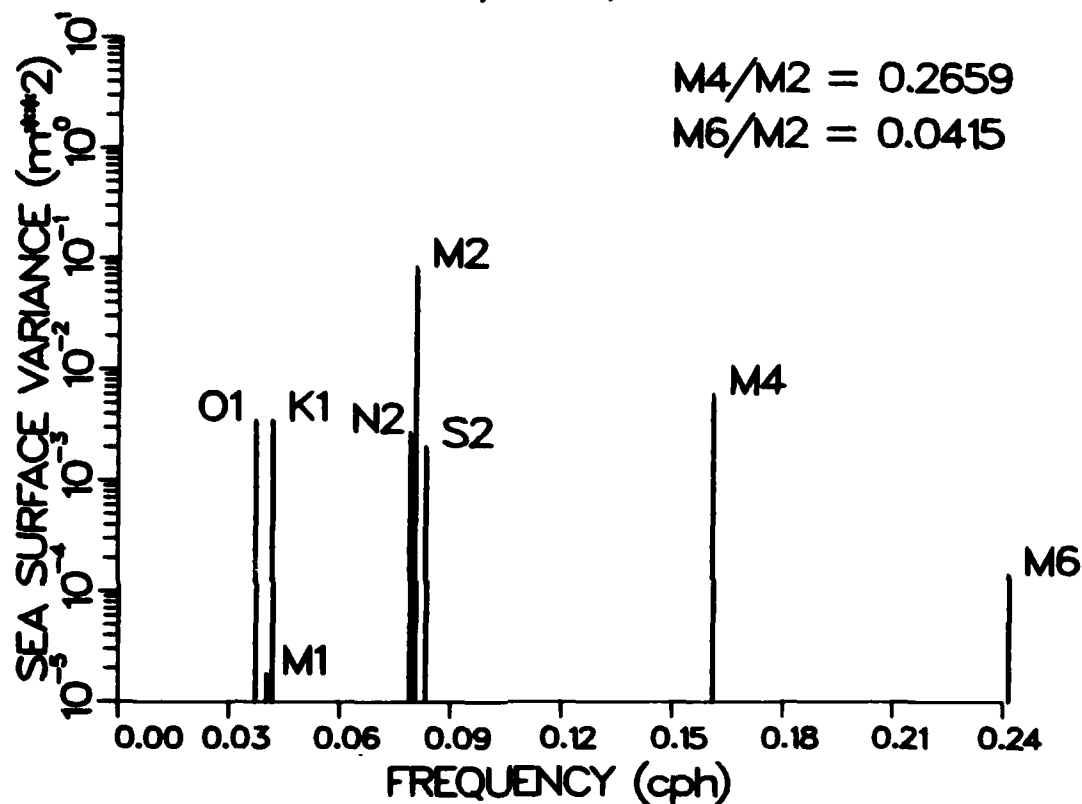
Figure 6.  Periodogram of tides within the estuary at Nauset Bay (location 8 in figure 3).
This station shows the most rapid growth of tidal non-linearities, and is the
most distorted of all tides measured in the estuary.  Tidal decay is also
greatest at this location.

TABLE 3

## TIDAL ASYMMETRY AT NAUSET

| STATION | DISTANCE FROM INLET | AVERAGE EBB | AVERAGE FLOOD |
|---------|---------------------|-------------|---------------|
| Ocean | ---- | 6 hrs. 13 min. | 6 hrs. 13 min. |
| Inlet | ---- | 6 hrs. 30 min. | 5 hrs. 57 min. |
| North Channel | 1.2 km | 7 hrs. 24 min. | 5 hrs. 01 min. |
| Nauset Bay | 2.0 km | 7 hrs. 43 min. | 4 hrs. 42 min. |
| Middle Channel East | 0.99 | 6 hrs. 46 min. | 5 hrs. 39 min. |
| Middle Channel West | 1.7 | 7 hrs. 00 min. | 5 hrs. 25 min. |
| Nauset Heights | 2.4 | 7 hrs. 03 min. | 5 hrs. 22 min. |
| Snow Point | 3.0 | 7 hrs. 12 min. | 5 hrs. 13 min. |
| Goose Hummock | 6.1 | 7 hrs. 32 min. | 4 hrs. 53 min. |

# NAUSET INLET/ESTUARY TIDES
## TIDAL DISTORTIONS
## OCTOBER–NOVEMBER 1982
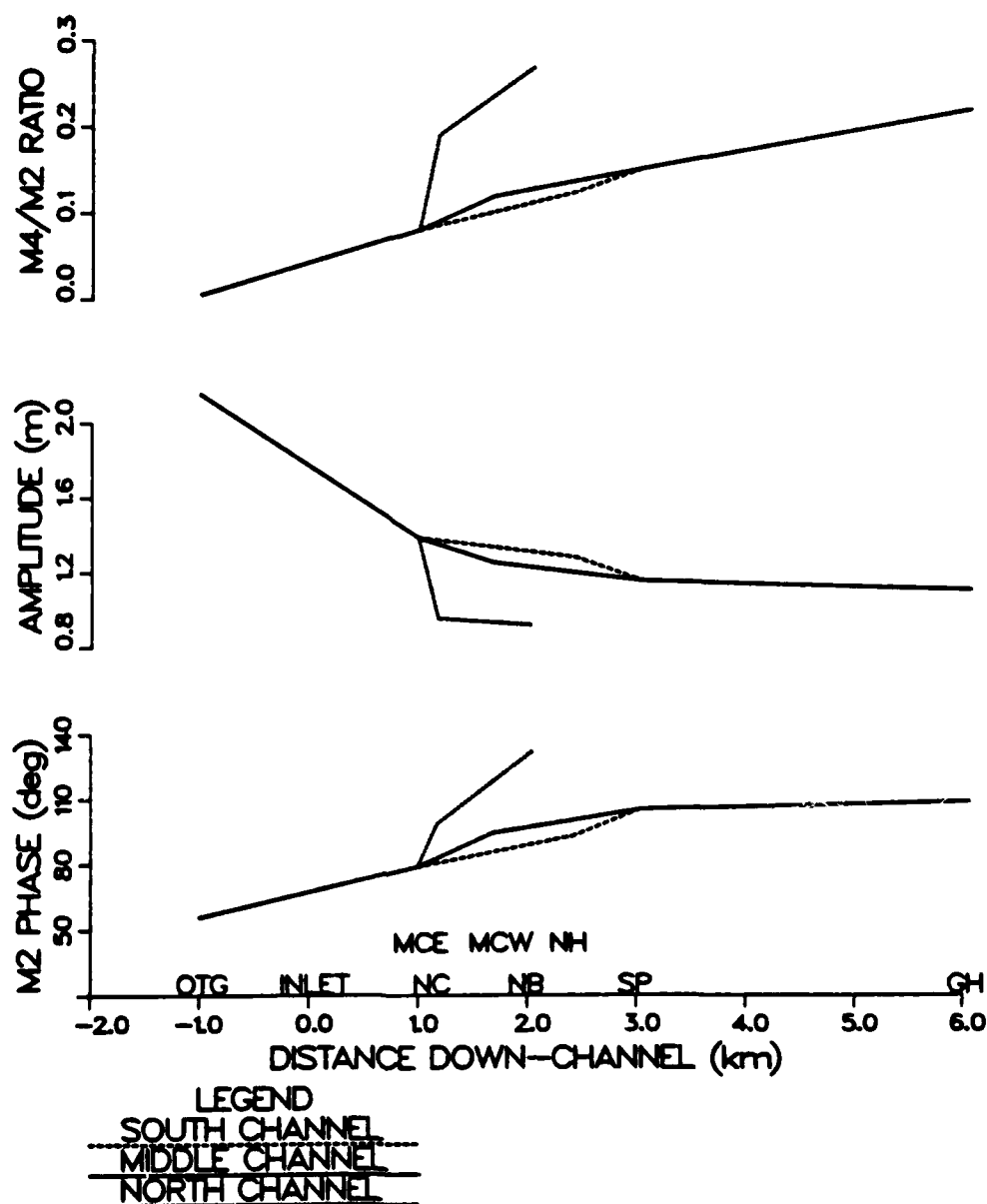


Figure 7.

Tidal distortion from the ocean proper through the three major channels of the estuary. Abbreviations for stations are as in figure 3. Top panel shows the increase in ration of $M_4/M_2$ tidal amplitudes with distance into the estuary. Largest ratio is in Nauset Bay, alon North Channel;. Second panel shows mean range of total tide as a function of distance into the estuary. Most rapid decay is along North Channel, least rapid decay is along South Channel. Lowest panel shows phase of $M_2$ tide throughout the estuary, referred to a local tidal epoch. Most rapid phase lags take place in North Channel, least rapid in South Channel.

# NAUSET INLET TIDAL FLOWS
## 30 AUGUST 1982
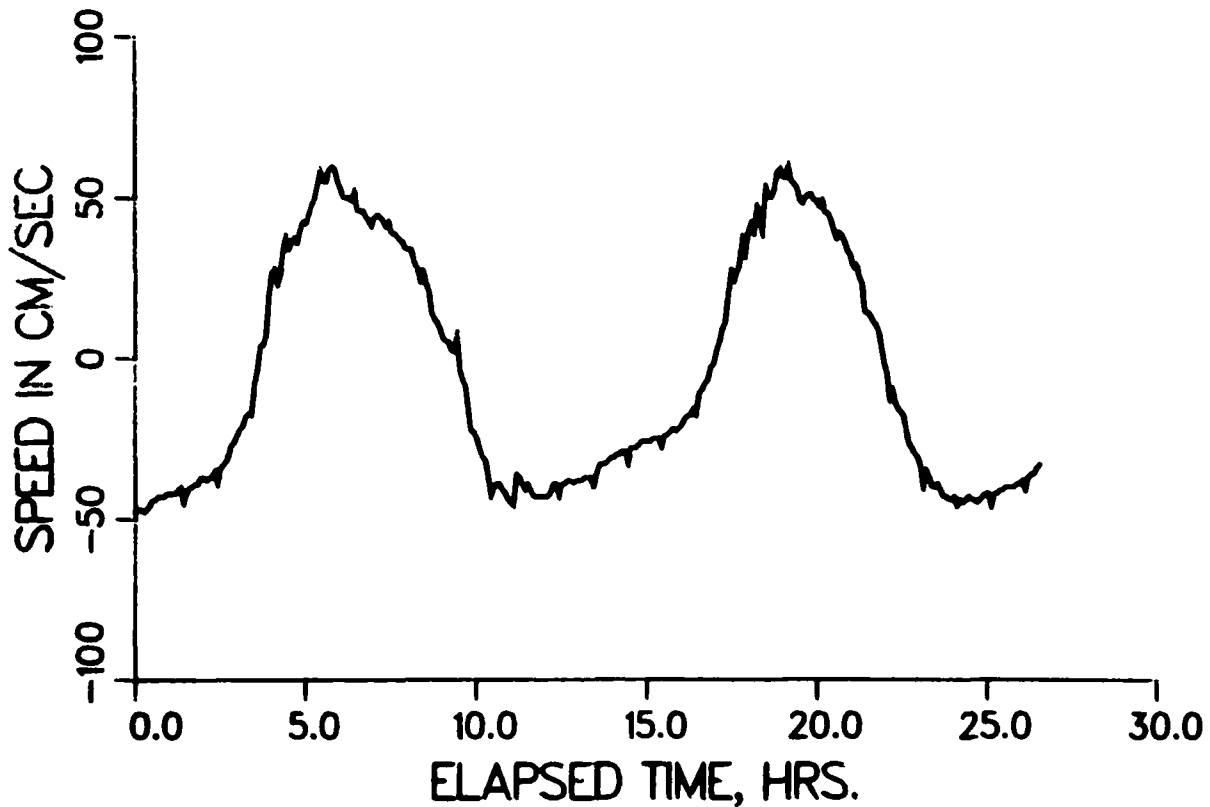


LEGEND
SENSOR 4

Figure 8.   Measurements of tidal velocity in the north part of South Channel (near Middle
            Channel East location) during the 1982 experiment.   Velocity is measured
            2.9 m above the bottom in water depth of approximately 3.5 meters, with a
            sample interval of 1 second.   Values shown in figure are three-minute averages,
            representing one of five sensors deployed at same location for same time period.

Field data collected from 1981 and 1982 clarify patterns of tidal distortion throughout the Nauset embayment. Using eight tidal locations distributed through Nauset Embayment (figure 3), both amplitude and phase relationships between $M_2$ and $M_4$ tides have been determined. All analyses shown cover the period 18 October through 16 November 1982. Additional harmonic analyses for more stations and different time periods are presented in Appendix 2. Six of the stations had measurements taken over that particular period of time; the final two were predicted from previous time series using harmonic prediction techniques (Schureman, 1971; Dennis and Long, 1971; Boon and Kiley, 1978). All records (measured and predicted) were analyzed using harmonic analysis (a least-square variant) to obtain phase and amplitude relationships for 25 components of the astronomical tide. Phases reported are local, referenced to the beginning of the time series, amplitudes are represented as root mean square tidal range for the time period in question.

Nauset embayment has three primary tidal channels of interest: South Channel, Middle Channel, and North Channel (figure 3). Tidal distortion can be shown schematically for these three primary channels, each of which has different bed roughness scales (sand waves, ripples), mean depth, and time-varying channel cross-sectional area. Consequently, terms in the momentum and continuity equations in each of the three systems have different magnitudes; the three channels give us an opportunity to evaluate model results from somewhat independent data.

North Channel gages exhibit the fastest non-linear down-channel growth (figure 7 and table 4). This channel exhibits the most rapid change in phase of $M_2$ along it's length, with a phase change of over 75° in a distance of two kilometers to Nauset Bay. Amplitude attenuation of the total tide over two kilometers is rapid, exceeding 55°/°. $M_4/M_2$ ratio increases 50-fold in two kilometers in this channel; $M_4/M_2$ ratios increase from a value of 0.005 in the ocean, to 0.27 at Nauset Bay.

-28-

TABLE 4

| Station | Distance From Inlet (km) | $M_2$(m) | $M_4$(m) | $M_4/M_2$ | $M_2$ Phase° | $H_{rms}$ |
|---|---|---|---|---|---|---|
| OCEAN* | -1. | 1.03 | 0.005 | 0.0049 | 55.7 | 2.15 |
| NORTH CHANNEL* | 1.17 | 0.441 | 0.083 | 0.188 | 98.7 | 0.95 |
| NAUSET BAY | 2.04 | 0.410 | 0.109 | 0.266 | 132. | 0.92 |
| MIDDLE CHANNEL EAST | 0.99 | 0.661 | 0.052 | 0.079 | 78.8 | 1.38 |
| MIDDLE CHANNEL WEST | 1.68 | 0.588 | 0.069 | 0.117 | 94.4 | 1.25 |
| SNOW POINT | 3.04 | 0.538 | 0.080 | 0.149 | 105. | 1.15 |
| GOOSE HUMMOCK* | 6.07 | 0.511 | 0.112 | 0.219 | 106 | 1.11 |
| NAUSET HEIGHTS | 2.42 | 0.601 | 0.073 | 0.122 | 93.0 | 1.28 |

\* Prediction from harmonic analysis, using constituents determined from different time periods.

Comparison is for 18 October to 16 November 1982.

Confidence limits for amplitude and phase are as given in Munk and Cartwright (1966). Confidence limits for variance are derived from $x^2$ distributions.

Middle Channel has greater mean depths than North Channel, and consequently a slower rate of non-linear tidal distortion. In approximately 3.0 kilometers of channel length to Snow Point, phase lags of $M_2$ are less than $50°$, as compared with more than $50°$ for North Channel in two Km. Amplitude attenuation is less, decreasing by about $45°/°$ over 3 km (versus greater than $55°/°$ in 2 km for North Channel), when compared to the open ocean tide. When compared to the tide immediately inside the inlet (at Middle Channel east), amplitude attenuation at Snow Point along Middle Channel is $17°/°$, as opposed to $35°/°$ at Nauset Bay along North Channel. $M_4/M_2$ ratio is about 0.15 at Snow Point, or thirty times that at the ocean station (compared to an increase of more than 50 times for North Channel). When referenced to the bay station nearest the inlet mouth, the $M_4/M_2$ ratio at Snow Point increases by a factor of two along Middle Channel, as opposed to a factor of more than three along North Channel.

South Channel is the least non-linear of the channels, because of a greater mean depth, and less channel curvature. Along its 2.4 km. channel within the bay, the phase changes approximately $°$ compared to the first bay station, and the amplitude attenuates approximately $40°/°$ compared to the ocean tide, or $8°/°$ from the bay station closest to the inlet mouth. Channel cross-sectional area is less variable over a tidal cycle here than the other two locations. This supports a hypothesis that tidal distortion is largely a result of time-varying channel geometry entering the equations of motion in both continuty and the frictional term in momentum. Local momentum balances along South Channel will be made from sea surface (pressure) gradient and velocity measurements in this area obtained in the 1981 and 1982 field experiments. Large amplitude sand waves in South Channel likely increase the importance of friction in this channel, but to a lesser extent than the distortion caused by channel area variability in the other two channels.

Locally non-linear tidal distortions appear from the field data to be caused the advective, frictional, and cross-sectional terms in the momentum and continuity equations. $M_4$ is consistently phase locked to $M_2$, with a lag of $63°$ (r.ms. deviation of $1.3°$). This phase-locking is another piece of information which helps pinpoint the dominant non-linear mechanism in these shallow estuarine systems.

As an example of the importance of the magnitude of $M_4$ relative to $M_2$ in determining tidal asymmetries, we show examples from two of our stations (figure 9). At the ocean station, ratio of $M_4/M_2$ is about 0.005. At the Nauset Bay site, this ratio is about 0.27. The ocean tide gage has equal peak ebb and flood elevations, and equal duration of flood and ebb. Nauset Bay, however, has a distinct asymmetry in flood and ebb, with a flood duration much shorter than the ebb duration. This will lead to increased maximum flood flows compared with ebb flows, resulting in generally larger flood sediment transport than ebb.

# NAUSET INLET TIDES
## TIDAL ASYMMETRY
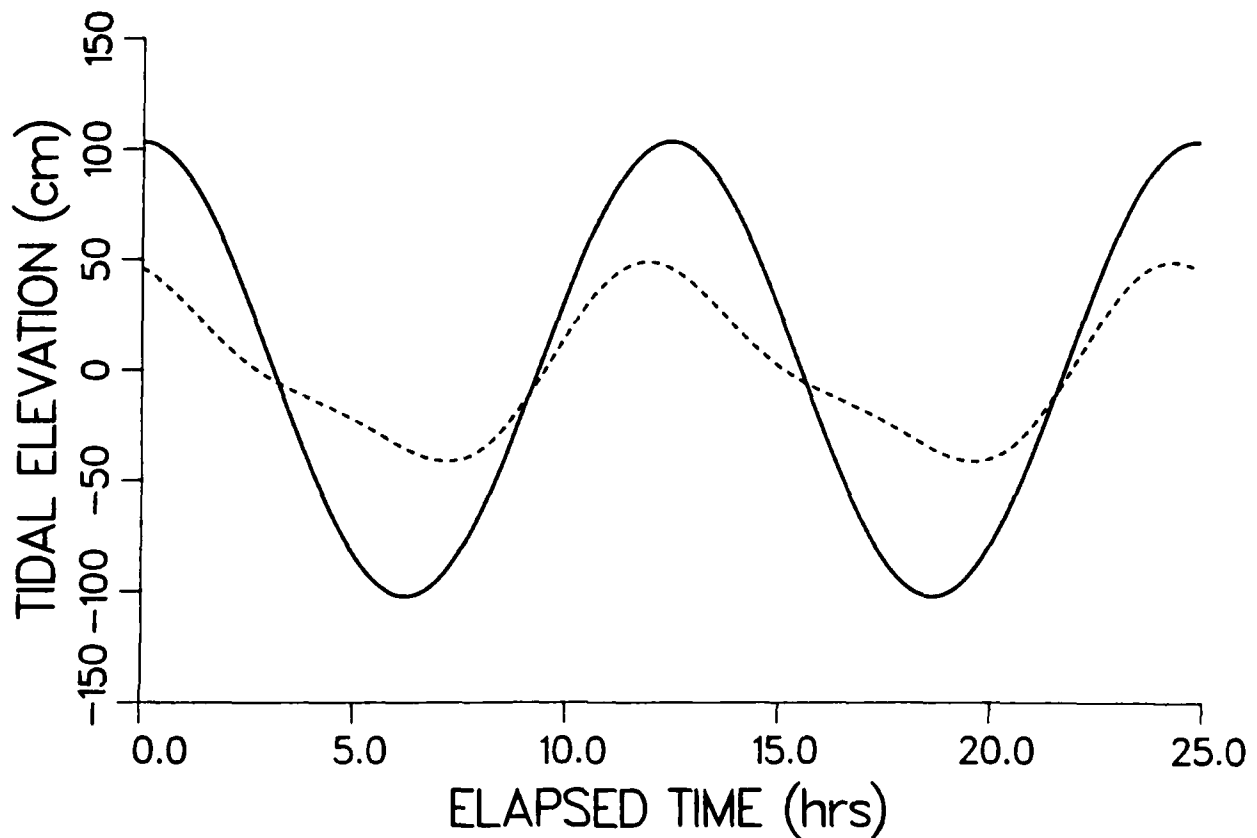


Figure 9. Nauset Bay and ocean tides formed from the $M_4$ and $M_2$ tidal constituents, with proper relative amplitudes and phases for the time periods shown in figure 4 and 6, illustrating the large distortion of the initially symmetric ocean tide after it propagates into the estuary.

Numerical Modeling:

The modeling involves use of explicit finite difference schemes in one-dimension (i.e., cross-sectionally averaged). Two-dimensional (depth-averaged) schemes have been employed where the flow can not realistically be considered one-dimensional. The models are used as diagnostic tools to examine the non-linear generating mechanisms. Models which include depth structure (3-D) are not used because of flow complexity introduced by shallow depths and large-scale bottom roughness. The numerics woud be greatly complicated without adding significantly to the physics of the problem. Since we are looking at the system's response to tidal forcing, the considerable averaging involved in the equations does not obscure the results. We want to determine the important mechanisms at any location and the rate of energy transfer to the harmonics, as well as the sediment transport implications for this estuary and how they differ from other systemsµ Model results are being compared spectrally with field results to examine the phase and amplitude of $M_2$, $M_4$, $M_6$, etc., and the growth of the harmonics caused by the various non-linear mechanisms.

These modeling goals require a careful approach to implementing open boundary conditions. As the system responds to tidal forcing, the various tidal harmonics generated in the estuary reflect to and radiate through the inlet, contaminating the measured pressure signal. Therefore, we are examining the response to $M_2$ forcing, and trying to separate the appropriate harmonic content introduced by the ocean as a boundary condition. We are also investigating the possibility of applying simple radiation conditions if they are needed (e.g., Reid and Bodine, 1968; Wurtele et al., 1971; Orlanski, 1975; Reid et al., 1977). The strong friction in these shallow systems may likely make this radiation condition unnecessary.

We take two basic steps in the numerical modeling. Initially, the estuarine system is idealized into its component channels and basins. Approximate dimensions and depths of these features are used with relatively simple geometry. We then study the effect of friction, advection of momentum and strongly time-varying channel/basin geometry on the tidal response of the system. Initially, the model results are examined for qualitative similarities with the actual system, i.e., right form and approximate magnitude of tidal asymmetry in both sea surface and velocity (figures 10 and 11). We then examine the results spectrally to see how the various non-linearities develop and interact within the system.

In the second phase of modeling, we input realistic geometry from the bathymetric data acquired in the field. Model sea surface elevations are compared spectrally with field measurements to examine spatial changes in harmonic content. This provides a good indication of how well the model reproduces an inherently non-linear physical system. Additionally, we can identify regions in the estuary displaying different rates of harmonic growth and assess the reasons. We are also studying the importance of friction in the system spectrally, and in terms of tidal amplitude and phase changes. These model results are then compared to field measurements. Finally, harmonic analysis applied to the terms in the equations of motion elucidates the sources of non-linearities in this more physically correct model (e.g., Prandle, 1980). Local momentum balances have been estimated from field measurements of pressure gradients and tidal transports.

Analytical Modeling:

As a means of evaluating numerical model results, we have implemented a limited analytical component. Initially, we are modifying the Kreiss (1957) model to reflect the scaling appropriate to Nauset Inlet and similar systems.
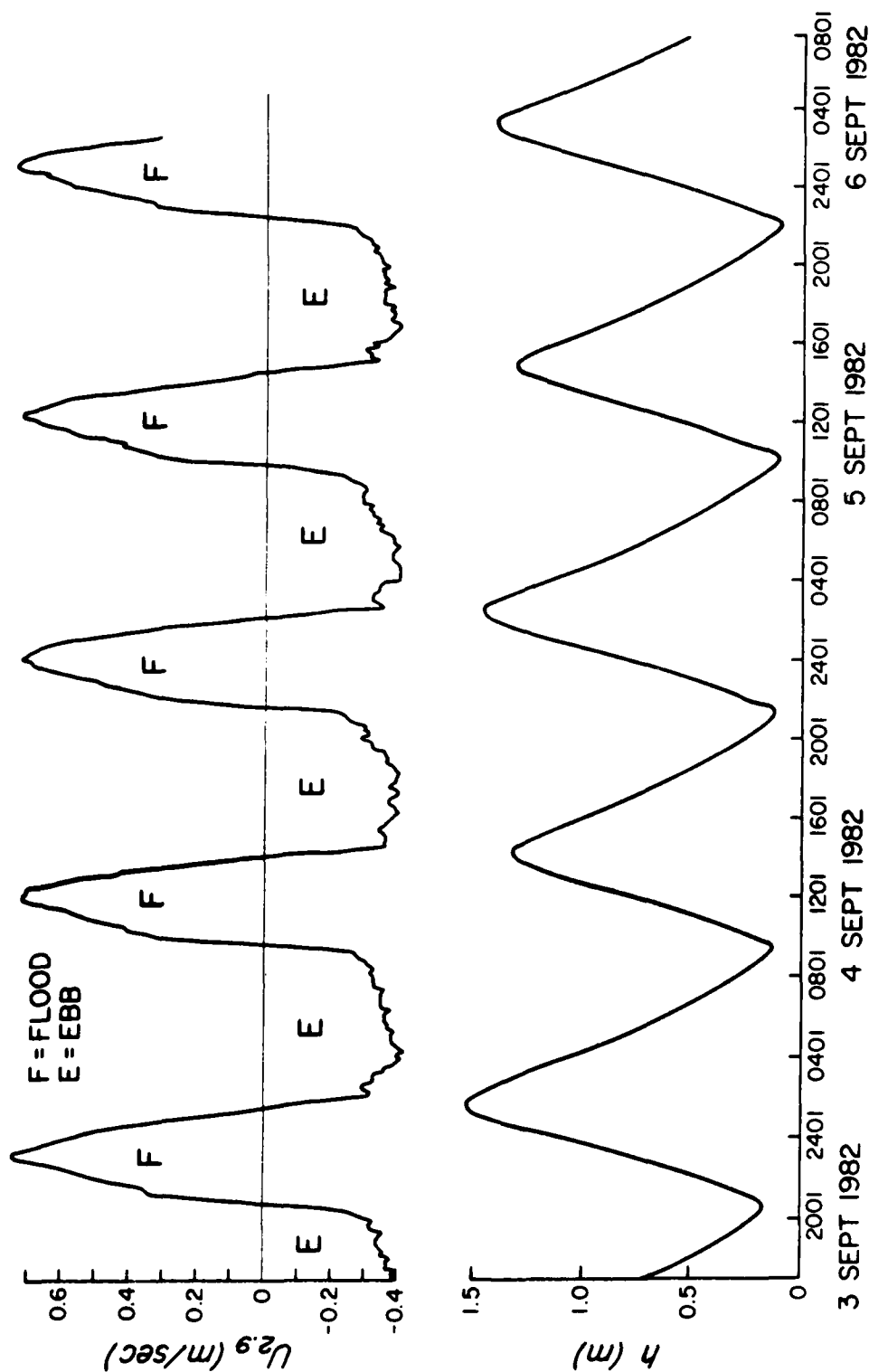
Figure 10

Measurements of velocity (top panel) and sea surface elevation (lower panel) for 2.5 days, acquired in the feeder channel leading into Town Cove (location 2 in figure 3). Velocity is that at top sensor (2.9 m above bottom in 3.5 m water depth) of five element array. Sea surface is with respect to arbitrary reference level. Our numerical models correctly reproduce these velocity and sea surface asymmetries, with the dominant non-linearities arising from friction and time-varying channel geometry.
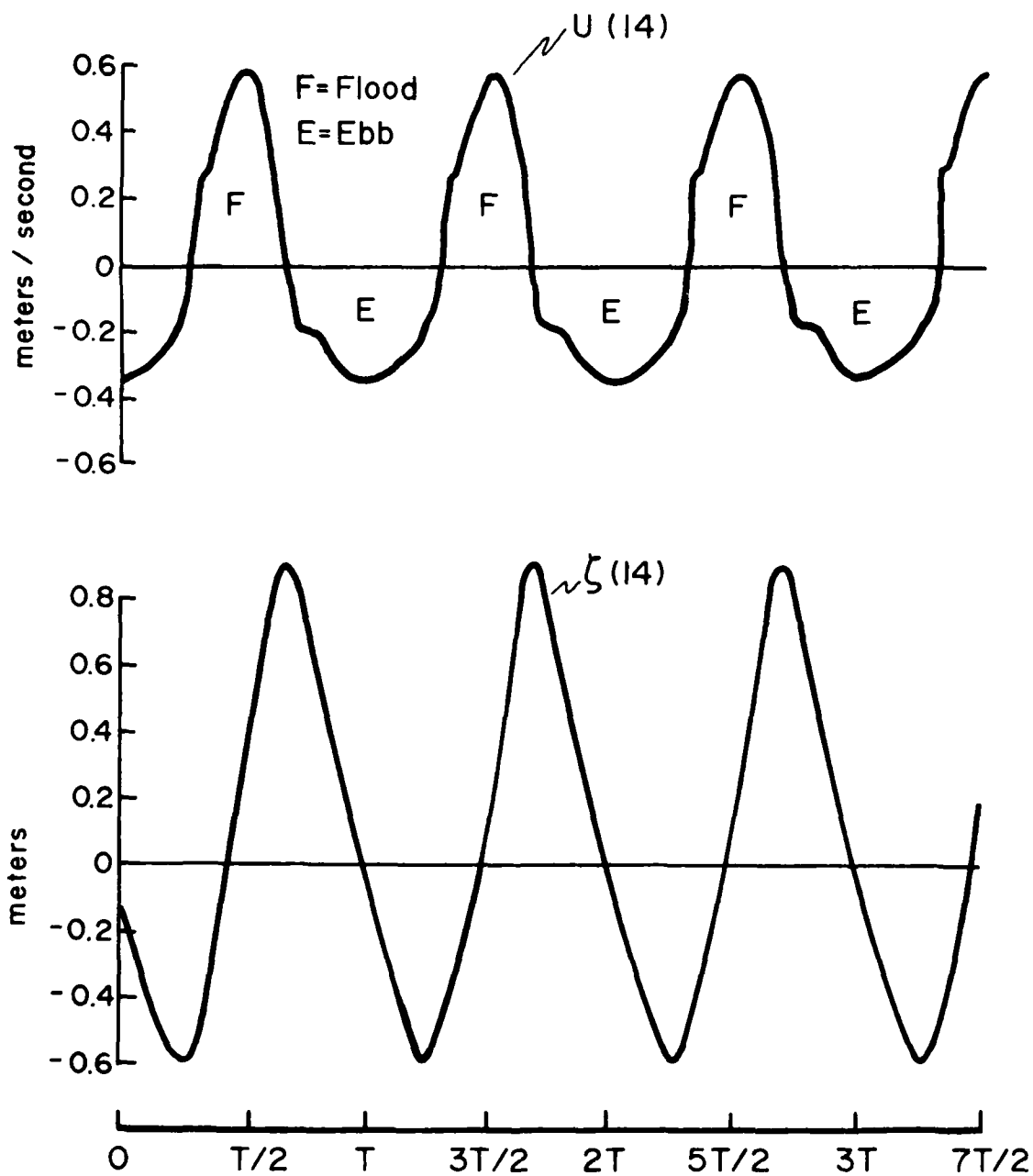
Figure 11. Predictions of near-surface velocity and sea surface elevation (upper and lower panels, respectively) for time period and location shown in figure 10. Calculations are from numerical model of tidal flows in this region.

In particular, velocity and length scales are redefined to develop a consistent perturbation series in the parameter a/h (a = tidal amplitude; h = mean depth; a/h <<1). Sea surface elevation and velocity are expanded in terms of this non-linear ordering parameter. As a second step, we are including simple models of time-varying channel cross-sectional area in continuity to evaluate its role in non-linear tidal distortion. In these models, channel width and cross-sectional area are expanded in terms of a/h. This work is in its early stages, so we have no results to present at this time.

TASK    2)    Effects of flow curvature on spatial non-homogeneity of tidal inlet flows, and resultant sediment transport: Casual observation of tidal inlet and estuarine flows shows that these channels often are not straight, but rather have pronounced curvature. This curvature has dramatic effects on flow through these channels, affecting near-bed shear stress distributions and resultant sediment transport. Complexity of channel geometry ranges from long, straight channels with occasional bends, to nearly continuous, sinuous geometry reminiscent of river channel meanders. Although probably not the dominant hydrodynamic control over tidal phase and amplitude distortion in inlet/estuarine systems, channel curvature locally controls flow patterns and resultant sediment transport. In addition, channel curvature near an inlet mouth may provide a mechanism for the inlet's migration (Task 3), a factor which provided the primary motivation for this part of the study.

In task 1, we relied heavily on one-dimensional representations of the flow field to investigate the problem of tidal distortion in shallow estuaries. The one-dimensional nature of the models, precludes explicit representation of channel curvature. Neglect of channel curvature does not appear to mask the dominant physics of tidal distortions, as indicated by numerical model results

presented in task 1. In fact, one-dimensional advection, non-linear friction, and time-varying channel geometry appear to thoroughly describe this non-linear harmonic growth to our desired degree of accuracy. Task 1 modeling does implicitly include effects of channel geometry through the frictional terms. Although local momentum balances calculated from field studies do not emphasize channel geometry, effects of flow curvature occurring along channel reaches are implicitly represented in friction estimates. Friction factors derived from our modeling efforts may not be entirely consistent with calculated friction factors assuming linear, uniform channels.

Our study of flow curvature is centered on channels near the inlet mouth rather than in distant estuarine channels. The study has included theoretical aspects of channel bend flows, and its application to inlet geometry at Nauset. A field program was directed towards evaluating the magnitude of the flow curvature effects within the tidal inlet at Nauset, using sea surface gradients as the primary diagnostic indicator. These measurements were then related to theoretical models.

Previous Work

An extensive literature discusses the effects of channel curvature on flow structure, largely resulting from an interest in river channel meanders and open channel flow. Much of the work to date has been done by engineers interested in channel scour and deposition, or by geologists studying riverine processes. Recently, more complete numerical models have quantified aspects of channel bend flow which had been described qualitatively by previous researchers.

The channel bend problem has been examined using different techniques: laboratory measurements, field measurements, analytical modeling, and numerical modeling. A recent, carefully-controlled series of laboratory

experiments was performed by Hooke (1975), who measured shear stress and sediment distribution in a channel bend. Excellent field measurements have been carried out by Dietrich et al. (1979) and Dietrich (1982), centered on a river meander of sufficiently small scale that accurate, comprehensive measurements were realistically possible. Analytical models of river bend flows generally cover only some limited aspects of the flow field (since the full three-dimensional flow is so complex). Examples of this modeling include Engelund (1974) and Bridge (1977), who generally assume simple bend geometry. Finally, numerical models have been recently applied to the problem of river bends, where more realistic channel geometry and more complete flow structure is considered. In particular, Nouh and Townsend (1979) considered a cylindrical bend, with a logarithmic vertical velocity profile. Leschziner and Rodi (1979) employ cylindrical polar coordinates with a turbulence closure model known as the "k-$\epsilon$" model, characterizing turbulence by the turbulent kinetic energy (k) and its rate of dissipation ($\epsilon$). Finally, Smith and McLean (1983) have proposed a model which uses curvilinear coordinates along-channel and cross-channel, allowing a continuously varying radius of curvature. A zero-order state defines the true channel depth so actual river meanders can be modeled. Convective accelerations are more properly modeled also, to yield better estimates of locally varying boundary shear stress. The latter model is the most complete for examining meandering streams, whether riverine or estuarine. Flows are considered steady in all of these models, so thereby limiting their application to non-steady tidal inlet and estuarine flows.

No numerical or analytical modeling is available which directly addresses non-steady flows in open tidal inlet/estuarine channels. The temporal acceleration term will not alter the general shear-stress distribution patterns found by other authors (e.g., Smith and McLean, 1983), but rather will modify these patterns through time.

## Modeling

Our analysis of tidal inlet flows in the presence of strong channel curvature is proceeds from a simplification of the Navier Stokes equations. The general form of these equations considered for the channel bend problem is:

$$\rho \frac{\partial u_i}{\partial t} + \rho u_j \frac{\partial u_i}{\partial x_j} = \frac{\partial p}{\partial x_i} + \frac{\partial \tau_{ij}}{\partial x_j} - \rho g \cos(g,i) \tag{1}$$

The Einstein summation convention is assumed in these momentum equations. Continuity is given as (for incompressible flow):

$$\partial(u_j)/\partial x_j = 0 \tag{2}$$

where  $u_i$ = velocity component

$x_i$ = spatial coordinate

$\tau_{ij}$ = deviatoric stress

$g$   = gravitational acceleration

$\cos(g,i)$ = cosine of angle between the gravity vector and the coordinate axis.

Specific application of this set of equations involves simplifying assumptions, and specification of an appropriate orthogonal curvilinear coordinate system. Whereas most investigators use a cylindrical coordinate system, Hooke (1975) and Smith and McLean (1983) employ a sine generated curve with varying radius of curvature, given by the equation:

$$\theta = \omega \sin 2\pi s/_L \tag{3}$$

where $\omega$ is the value of $\theta$ at ($^{2\pi s}/L = {}^{\pi}/2$), L is the wavelength of the center-line meander, and s is down-channel axis. $\theta$ is curvature of the centerline. The variable radius of curvature, R, is simply given as:

$$R = (\frac{\partial \theta}{\partial s})^{-1} = (\frac{2\pi\omega}{L} \cos \frac{2\pi s}{L})^{-1} \tag{4}$$

Additional simplification of the equations of motion include depth averaging and specification of the form of the deviatoric stress tensor. This normally occurs by scaling the equations of motion in a consistent fashion, and examining lowest order solutions to that suitable expansion scheme.

Some insight into channel bend flow can be derived from these simplified forms of the equations of motion. For instance, the downstream momentum equation can be simplified considerably along the centerline in the case of zero flow divergence and quasi-steady flow to:

$$0 = +\rho g \, \partial \eta / \partial x + \partial \tau_{xz} / \partial z$$

so

$$\tau_{xz} = -\rho g \left( \frac{\partial \eta}{\partial x} \right)(h-z) \tag{5}$$

where $\partial \eta / \partial x$ is the downstream slope, and $\tau_{xz}(z = h) = 0$.

Bottom stress is calculated for $z = 0$ as:

$$\tau_b = -\rho g h \, \partial \eta / \partial x \tag{6}$$

This equation provides a simple stress balance in the downstream direction, yielding a bottom shear stress estimate from a downstream sea surface gradient.

The lowest order equation for cross-stream flow is:

$$\frac{U^2}{R} = -g \frac{\partial \eta}{\partial n} + \frac{1}{\rho} \frac{\partial}{\partial z} \tau_{nz}$$

where n is the cross-stream coordinate, R is the radius of curvature, and U is the downstream centerline velocity.

If the friction velocity is much less than the mean velocity, and the channel half-width b is much less than the radius of curvature, then:

$$\frac{U^2}{gR} = \frac{\partial}{\partial n} (\eta) \tag{7}$$

But, for $\frac{1}{R} = \frac{1}{R_0} \cos \frac{2\pi s}{L}$ for a sinusoidal channel, then

$$\frac{U^2}{gR_0} \cos \frac{2\pi s}{L} = \frac{\partial}{\partial n} (\eta)$$

This can be integrated to yield:

$$\eta = \eta_0 + \frac{n}{gR_0} U^2 \cos \frac{2\pi s}{L} \tag{8}$$

where $\eta_0$ = reference elevation. We can calculate $\eta$ at $n = \pm b$, and determine the difference $(\eta_b - \eta_{-b})$ at $s = 0$, the point of maximum channel curvature:

$$(\eta_b - \eta_{-b}) = \frac{2b}{gR_0} U^2 \tag{9}$$

This is an approximation to the cross-channel set-up. $U^2$ can be calculated from $\tau_b$, assuming:

$$\tau_b = \rho C_f U^2. \tag{10}$$

where $C_f$ is a friction coefficient.

then:

$$(\eta_b - \eta_{-b}) = \frac{2bh}{R_0 C_f} \partial \eta / \partial x \tag{11}$$

Alternative methods for making this calculation exist, including use of eddy viscosity models for turbulent closure (see, for example, Engelund, 1974), and more complete perturbation expansions are available in the literature (e.g., Smith and McLean, 1983), particularly for calculating higher order velocity terms.

## Results

As in many tidal inlet/estuary systems, channel curvature can play an important role in local patterns of sediment transport. Nauset Inlet, as discussed previously, is formed of a number of relatively straight channels (figure 1), interconnecting at various angles resulting in channel bends.

Morphology of sand bodies near these bends is similar to that in many river bends: on the inside of the bend a point bar exists with bedforms actively migrating across. On the outside of the bend, a deeper pool is developed; these pools are the deepest sections within the channel network serving the estuary. Although for our tidal distortion modeling we ignore the localized effects of channel bends with some theoretical justification, local sediment transport patterns can be dominated by this flow distortion. The analogy with river bends is incomplete for a number of reasons. First, the flow is not steady but rather quasi-steady with a period of 12.42 hours. This period is much shorter than typical time scales of unsteadiness in rivers. Over certain portions of the tidal cycle, inertial effects therefore cannot be ignored. Second, river bends typically have a spatial periodicity represented by some representative wavenumber, $\lambda$. This spatial periodicity gives rise to distorted flows leading into subsequent river bends. For the tidal channel case, the flow coming into a bend is often much more uniform since the flow is arriving from a straight channel or large tidal basin. In some cases, however, flow into these bends is highly distorted due to a non-periodic spatial distribution of channel curvature. An alternative way of modeling the tidal channel flow would be a full depth-averaged two-dimensional model, similar to the river bend model of Smith and McLean (1983), only with unsteady flow and for aperiodic channel morphology.

As a means of determining the degree of flow curvature caused by curvilinear channel morphology, limited experiments on sea surface gradients were conducted. We attempted to examine spatial structures of the horizontal velocity field, but the difficulty of making velocity profiles in a tidal channel with rapid flows and large bedforms made interpretation of these results difficult.

Experimental procedure consisted of measuring down-channel and cross-channel sea-surface slopes, using pressure sensors with accuracies of 1 cm or better. Channel geometry was defined from stereo vertical aerial photographs of mapping quality, from which figure 2 is largely derived. Local bottom morphology and bathymetry were determined from precision bathymetric profiling, while relative sensor locations were determined from microwave navigation and vertical leveling when possible.

Vertical photographs from 21 September 1981 and 22 August 1982 were used to define the large scale morphologies of the channel bend forming the inlet proper (figure 2 and Table 5). Although some investigators have used the empirical observation that the radius of curvature in a bend varies as a sine-generated curve, for our purposes we have approximated the channel bend as a sector of a circular arc, with parallel channel banks. Because we are investigating the effects of isolated bends, not a number of bends in series, this approximation is reasonable for most of a tidal cycle. Angular extent is defined as the angle subtended by the curvilinear channelized portion of the flow during low tide. Low-tide channel widths are averages over the angular extent defined above for low water. Radius of curvature is constant through the bend, as defined earlier, and extends to the centerline of the channel.

Down-channel pressure gradients are available from two sets of measurements: one from 1980 and one from 1982. The 1980 measurements cover five days of data, so they will be discussed here (figure 12). Separation between the two pressure sensors used in the analysis was 425 meters, and the sensors were aligned along the approximate centerline of the channel over the deepest section of the channel. Measurements may be contaminated by along-channel variation in cross-channel set-up, but since the radius of curvature of the channel is constant, this error should be small. Maximum surface

-44-

## TABLE 5

|        | 21 SEPT 1981 | 22 AUG 1982 |
|--------|--------------|-------------|
| $R$    | 150 m        | 160 m       |
| $2b_{low}$ | 60 m     | 60 m        |
| $\theta_{sub}$ | 140° | 150°        |

Channel geometry derived from vertical aerial photographs of study area. $R$ is the centerline mean radius of curvature, $2b_{low}$ is the low-tide channel width, and $\theta_{sub}$ is the arclength subtended by the curved portion of the channel at low tide.
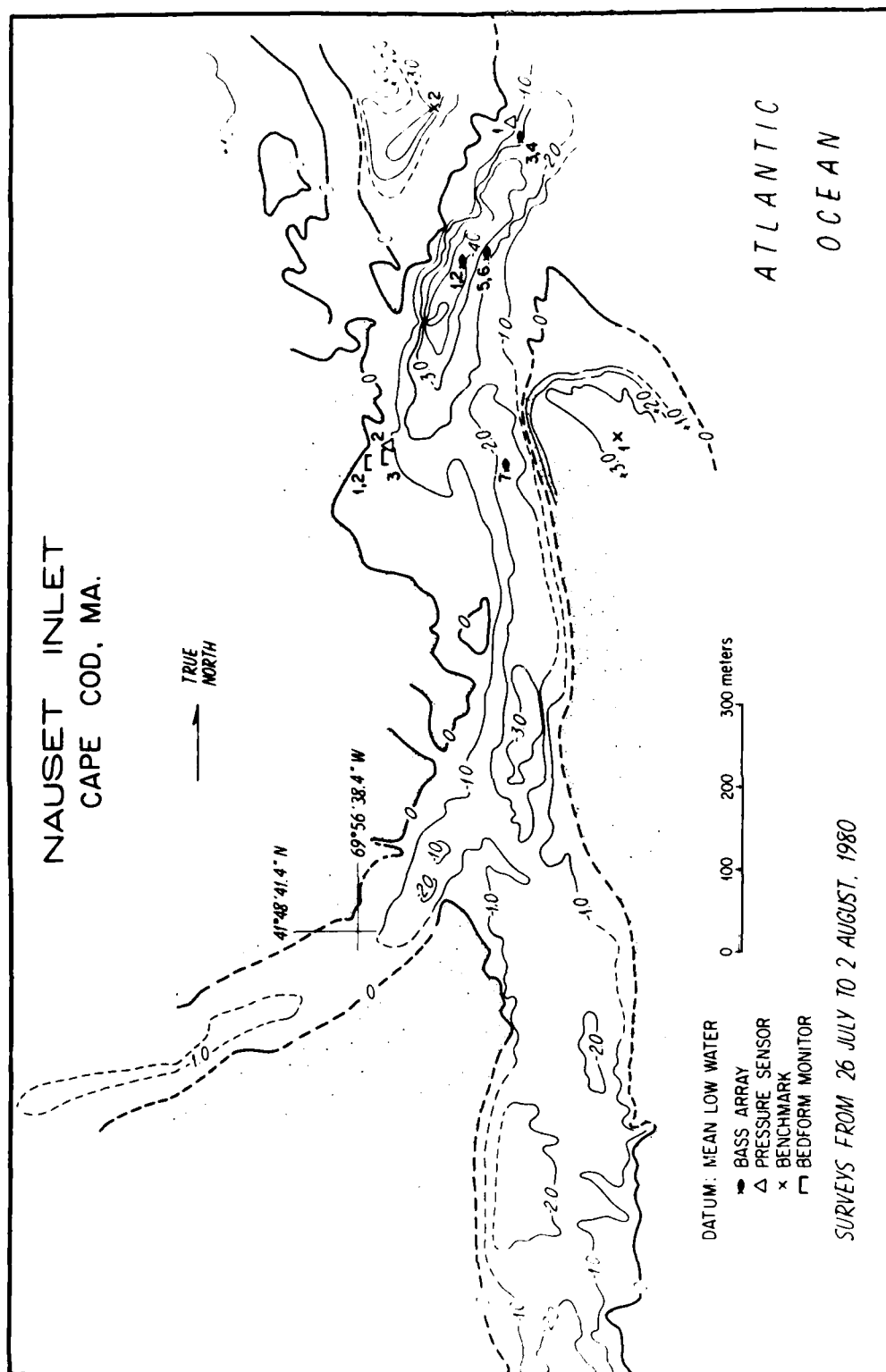
Figure 12. Location of equipment for 1980 Nauset Inlet experiment, which was a shake-down for later, more intensive experiments.

-46-

gradients occur late during flood and late during ebb tides, after mid-tides
(figures 13 and 14).  Maximum ebb tide gradients are greater than flood tide,
reaching values of 0.0007 (thirty centimeters over the channel length
separating the two sensors).  Maximum flood tide gradients are lower than ebb,
reaching 0.0005 (twenty centimeters over the separation).  Average maximum set-
up and set-down over the five-day period is nearly the same for flood and ebb
tide (18.5 cm).  During ebb tide, following mid-tide, sea surface elevation at
any particular station has a distinct knee (or change of slope, figure 13).
The position of this knee reflects the time-varying channel geometry (through
the hypsometric curve), whereby most ebbing flow becomes confined to the
narrow,deeper part of the main inlet and estuarine channels.  Constriction of
this cross-sectional drainage area results in maximum ebb velocities, hence in
maximum downstream sea surface gradient.  A similar knee does not occur during
flood tide, because flow velocities are relatively lower during early flood
compared to late ebb.

From equation 6, maximum near-bottom shear stress estimates can be calculated:
At maximum ebb flow:

$$\tau_b = -\rho g h \; \partial\eta/\partial x = -(1.0)(981)(200)(-0.0007)$$

$$\simeq 140 \text{ dynes/cm}^2$$

At maximum flood flow:

$$\tau_b = \rho g h \; \partial\eta/\partial x = (-1.0)(981)(300)(-0.0005)$$

$$\simeq 140 \text{ dynes/cm}^2$$

These estimates are averaged over channel length, as well as over channel
width.  Bottom shear stress calculated is total bottom shear stress, including

BAY PRESSURE SENSOR
NAUSET INLET
JULY 27 - AUGUST 1 , 1980
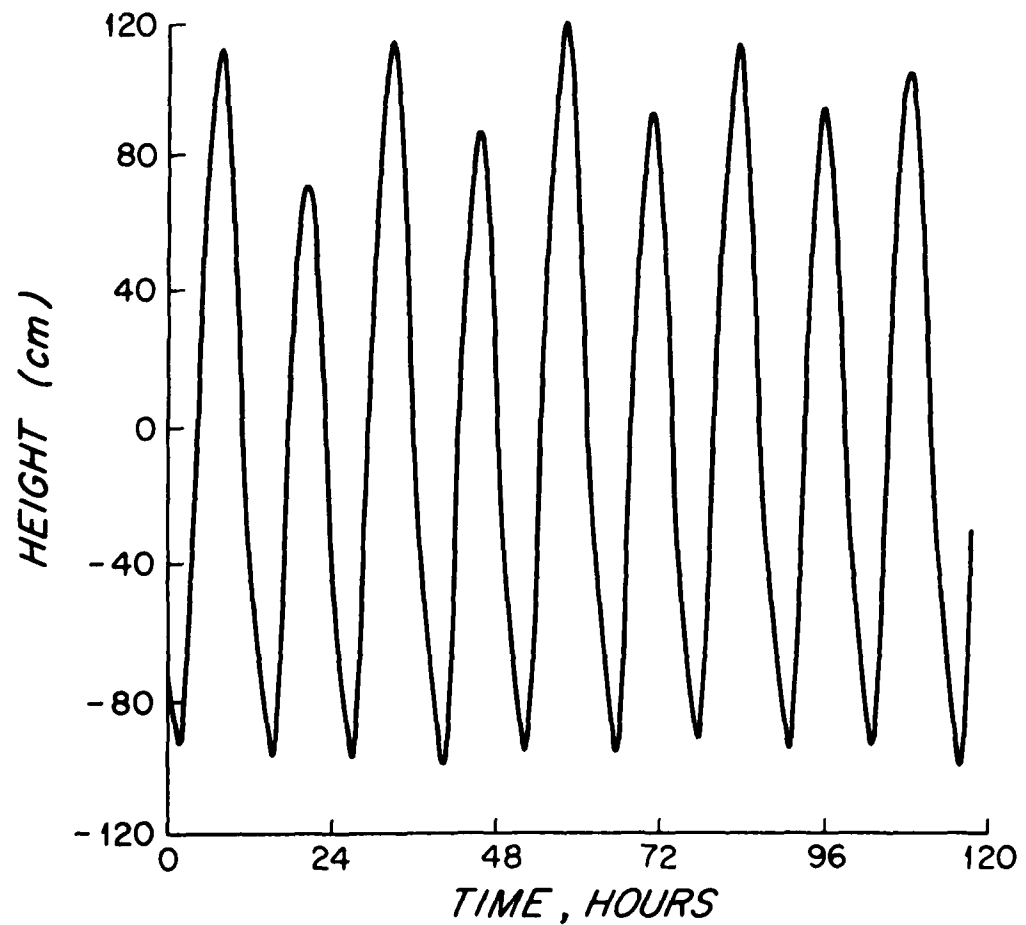
Figure 13.  Sea surface elevation measured by pressure sensor at location shown in figure 12, over period of the study.  Tidal amplitude was nearly 2 m at time of these measurements.

**BAY P/S — OCEAN P/S**
**NAUSET INLET**
**JULY 27 - AUGUST 1 , 1980**
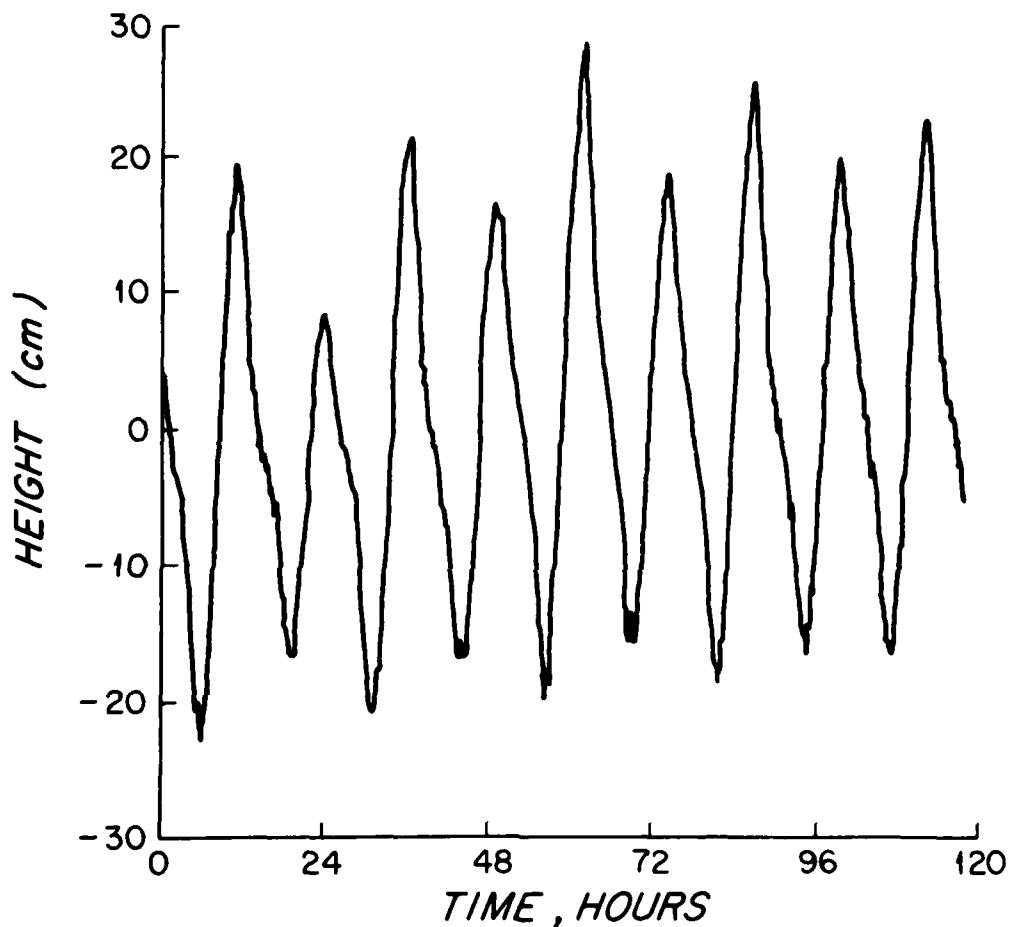


Figure 14.  Sea surface elevation differences for two along-channel pressure sensors
(see figure 12 for locations) during period of 1980 experiment.  Separation
of two sensors was approximately 400 m.  Maximum sea surface difference
was nearly 30 cm; average of peak set-down was 18 cm over the duration of
the study. Water level datum is arbitrary.

the effects of skin friction, form drag, wave-current frictional interactions and sediment transport (e.g., Grant and Madsen, 1981).  It is not a simple task to separate near bed shear stress (skin friction) for sediment transport purposes from this total bed shear stress estimate.

Using equation 11, we can estimate the cross-channel set-up:

$$(\eta_b - \eta_{-b}) = \frac{2bh}{RC_f} \; \partial\eta/\partial x$$

For h = 200 cm, $\partial\eta/\partial x$ = 0.0007, $C_f$ = 0.01, R = 1.5 x $10^4$ cm, 2b = 6 x $10^3$ cm,

$$(\eta_b - \eta_{-b}) = 5.6 \text{ cm}$$

For the same parameters except $C_f$ = 0.05:

$$(\eta_b - \eta_{-b}) = 1.1 \text{ cm}$$

For h = 300 cm, $\partial\eta/\partial x$ = 0.0005, $C_f$ = 0.01, R = 1.5 x $10^4$ cm, 2b = 6 x $10^3$ cm,

$$(\eta_b - \eta_{-b}) = 5.6 \text{ cm}$$

and for $C_f$ = 0.05, $(\eta_b - \eta_{-b})$ = 1.1 cm

Cross-stream sea surface slope becomes, for the case of $\Delta\eta$ = 5.6 cm, $\partial\eta/\partial n$ = 0.0009, of similar magnitude as downstream gradients.

Equation 10 can be used to calculate $U^2$, and hence U:

$$U = \sqrt{\tau b/_\rho C_f}$$

For $C_f$ = 0.01:

$$U = 118 \text{ cm/sec}$$

For $C_f$ = 0.05:

$$U = 53 \text{ cm/sec.}$$

For maximum ebb flow, the cross-sectional averaged velocity (3 minute-average) is approximately 0.7 - 1.0 m/sec, so a friction factor estimate of $C_f = 0.01$ to 0.03 is a reasonable value.

These calculations show the expected maximum cross-channel set-up to be of the order of 0.05 m, easily resolvable by our pressure sensors. To evaluate the cross-channel set-up, we emplaced an array of pressure sensors during NI-82 across channel near the inlet mouth (figure 3). Because of the difficulty of precisely determining the cross-channel coordinate in the field, the set-up signal is expected to have some downstream gradient contaminating the cross-channel measurement.

Results from this two-day field experiment show a complicated structure in set-up, consisting of a superposition of downstream and cross-stream set-up (figure 15 and 16). Set-up values were averaged over one-half hour to reduce the high-frequency noise in the data, reflecting short-period flow disturbances and, to some extent, surface wind wave activity. Internal pressure sensor processing removed most of this surface wind wave activity before recording, so this did not overpower the set-up signal. The cross-channel set-up is masked by other time-varying superelevation signatures, whose exact hydrodynamic source is unknown at this time.

Set-up at maximum tidal flows (the latter estimated from records of pressure change ($\partial \eta/\partial t$) without including effects of hypsometry or flow inertia, figure 17), show structures with a magnitude of five-to-eight cm, superimposed on some broader set-up event. Efforts to separate out these sources of set-up were not completely successful. Along-channel set-up was eliminated using phase and amplitude relationships between sea surface height and along-channel pressure gradient established from measurements taken during

# SET—UP ACROSS NAUSET INLET
## 3—4 SEPTEMBER 1982
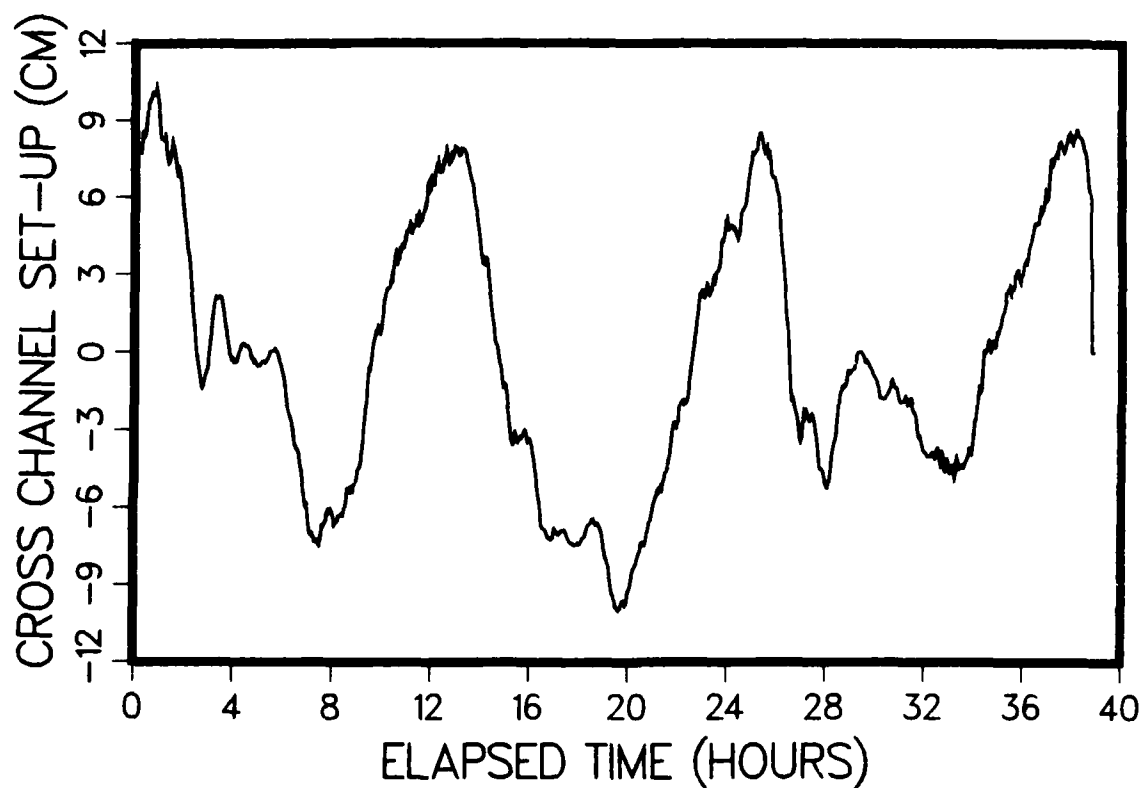


Figure 15.  Cross-channel tidal elevation differences measured during 1982 Nauset experiment, with sensors separated by 60 meters.  This time series is the raw elevation difference averaged over one-half hour intervals between two cross-channel sensors. Water level datum is arbitrary.

# NAUSET INLET TIDES
## 3–4 SEPTEMBER 1982
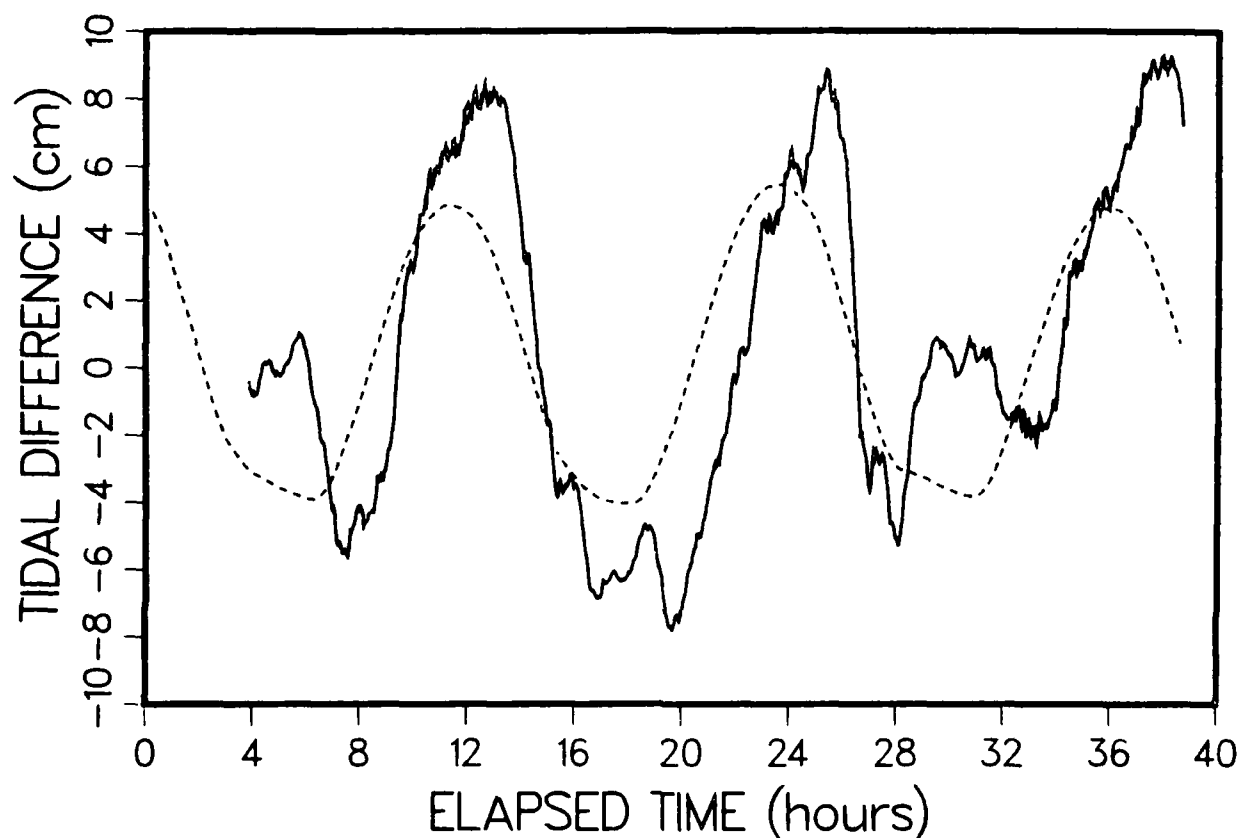


Figure 16.   Sea surface elevation differences as in figure 15, only with the along-channel set-down subtracted from the raw differenced signals.   Down-channel differences were predicted from relationships derived during the 1980 and 1982 experiments, and based on the along-channel component of the separation between the two instruments.   Dashed line is a scaled-down plot of sea surface, shown for its relative phase information.

# NAUSET INLET TIDES
## 3-4 SEPTEMBER 1982
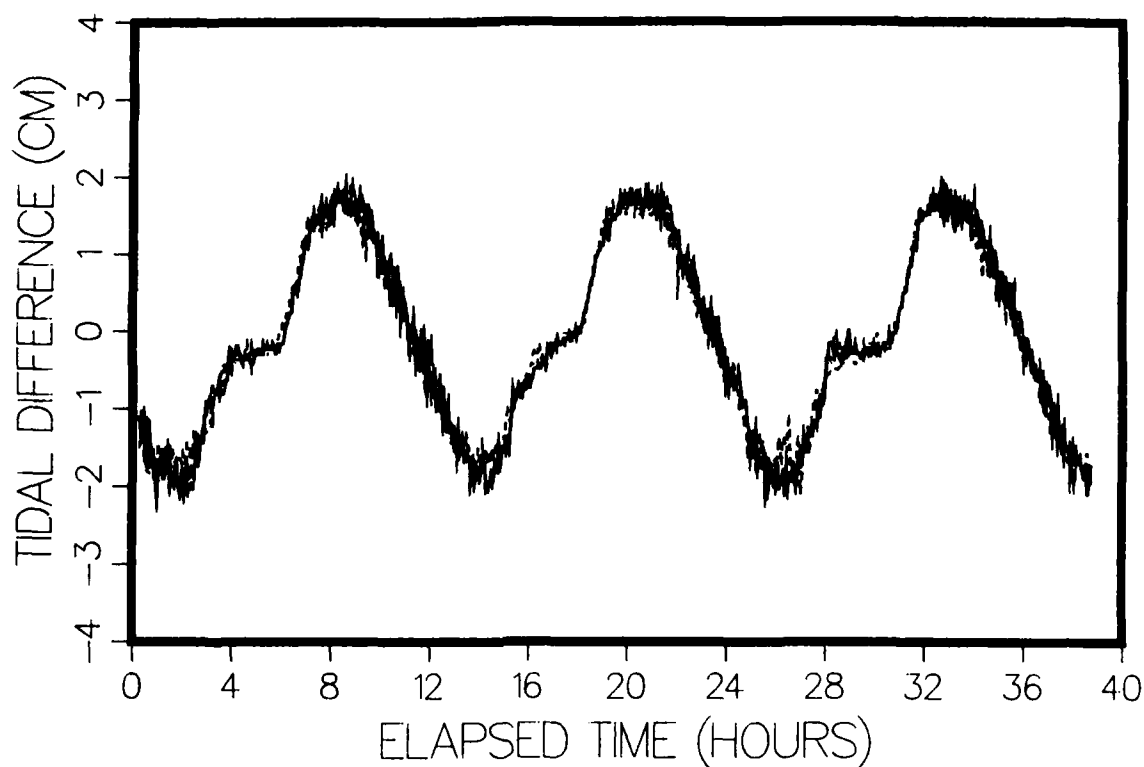


LEGEND
NORTH INLET TIDE GAGE
SOUTH INLET TIDE GAGE

Figure 17. Time-derivative of sea surface elevation at two cross-channel pressure
sensors for the 1982 experiment, showing the approximate form of the
expected velocity signal for the inlet during the period of the cross-
channel measurements (no velocity data were acquired at this location
during this short experiment). If a hypsometric curve typical of
Nauset estuary were included in this figure, the true velocity curve
would be well-approximated.

both NI-81 and NI-82. The component of downstream set-up contributing to the cross-channel measurements was then removed (figure 16). The resulting set-up incorporates elements consistent with our simple model of channel-bend flows, with magnitudes of 6 cm, but also includes energetic elements which are not explained by our simple model, occurring near high tide. Calibration of the pressure sensors and consideration of sources of instrument noise show that this set-up is real, and not a measurement artifact.

## Discussion

To increase our understanding of tidal flows through inlets, we have attempted some simple modeling based on ideas similar to river-bend flow structure. The model is only approximate for several reasons:

Tidal flows are quasi-steady at best.

Tidal channel bends are generally not as periodic as river bends.

Tidal inlet cross-sectional areas are strongly dependent on tidal stage.

With these and other constraints in mind, field observations of tidal inlet flows were examined using these flow curvature models. Results show that flows through inlet channels have strong friction ($C_f$ = 0.01-0.03), composed of near-bed shear stresses, form drag over large bedforms, and possibly considerable sediment transport effects. Maximum sustained (3 minute) depth-averaged tidal flows are near 75-100 cm/sec. These result in along-channel and cross-channel gradients of up to 0.007 at times of maximum flows. If flow expansion is allowed to take place (at ebb tide, for instance), the magnitude of these gradients can be increased. All measurements in this study were undertaken in regions where flow expansion is relatively unimportant over most of the tidal cycle.

Cross-channel set-up due to flow curvature effects are observed in field measurements, although they are superimposed on an energetic sea surface signal of unknown hydrodynamic origin.

This flow curvature results in a highly three-dimensional bottom stress distribution, similar in some aspects to steady river bend flow (see Hooke, 1975, and Dietrich et al., 1979, for example). The bottom shear stress pattern at Nauset results in a strong tendency for northward inlet migration. Implications of this tendency are discussed in greater detail under TASK 3.

Future work anticipated for this flow curvature study includes numerical modeling of these environments considering unsteady flows, time-varying cross-sectional channel areas, aperiodic channel bends, and other more realistic channel features.

TASK    3)    Clarification of mechanisms for updrift migration of natural, unstructured tidal inlets: One manuscript has been completed on this topic, and submitted to the Geological Society of America for publication. We are presently modifying the text in response to reviewers' comments. The manuscript, titled 'Updrift migration of tidal inlets: a natural response to wave, tide and storm forcing', written by D.G. Aubrey, P.E. Speer, and E. Ruder, describes three mechanisms for inlet migration, which can result under certain conditions in a net migration counter to the direction of longshore sand transport. The abstract of the paper follows:

Three mechanisms are responsible for tidal inlet migration in an updrift direction (counter to net longshore transport): 1) attachment of distal ebb tide delta bars to the downdrift barrier spit; 2) storm-induced breaching and subsequent stabilization to form a new inlet; and 3) ebb tide discharge around a sharp channel bend creating a three-dimensional flow pattern which erodes

the outer channel bank and extends the inner channel bank. The last two
mechanisms can result in either updrift or downdrift inlet migration, depending
on channel geometry in the bay and barrier beach configuration. Analysis of
historical charts and aerial photographs, combined with an historical storm
synthesis, shows that all three mechanisms are active at a natural tidal inlet
along a sandy coast (Nauset Inlet, Cape Cod, MA). On a time scale of ten
years, these mechanisms were effective in producing an updrift migration of
more than two kilometers.

TASK    4)    Hypothesis of mechanisms by which barrier beaches can elongate
under conditions of minimal longshore sand transport: In the course of our
investigations of tidal inlet and barrier beach behavior, a peculiar inlet
migration episode was observed with no obvious relationship to conventional
descriptions of barrier beach elongation/tidal inlet migration. A model was
proposed to describe this situation, suggesting that peculiar geometry of the
barrier beach overlapping the adjacent shoreline caused ebb tidal flows to
lengthen the inlet channel, depositing the eroded material as a marginal inlet
shoal, which added to the length of the barrier spit. The model is described
in a paper by Aubrey and Gaines (1982), titled 'Rapid formation and degradation
of barrier spits in areas with low rates of littoral drift'. The abstract of
that paper follows:

A small barrier beach exposed to low energy waves and a small tidal range
(0.7 m) along Nantucket Sound, MA, has experienced a remarkable growth phase
followed by rapid attrition during the past century. In a region of low
longshore transport rates, the barrier spit elongated approximately 1.5 km
from 1844 to 1954, developing beyond the baymouth, parallel to the adjacent

Nantucket Sound coast. Degradation of the barrier spit was initiated by a succession of hurricanes in 1954 (Carol, Edna and Hazel). A breach opened and stabilized near the bay end of the one kilometer long inlet channel, providing direct access for exchange of bay water with Nantucket Sound, and separating the barrier beach into two nearly equal limbs. The disconnected northeast limb migrated shorewards, beginning near the 1954 inlet and progressing northeastward, filling the relict inlet channel behind it. At present, about ten percent of the northeast limb is subaerial: the rest of the limb has completely filled the former channel and disappeared. The southwest limb of the barrier beach has migrated shoreward, but otherwise has not changed significantly since the breach.

A new mechanism is proposed for spit elongation when the inlet thalweg parallels the beach axis, in which material scoured from the lengthening inlet is the dominant source for spit accretion (perhaps initially deposited as a linear channel-margin bar which later becomes subaerial). The lengthening spit causes the parallel inlet to elongate, which in turn further lengthens the spit, in a self-generating fashion. This mechanism provides both a source of sediment for elongating the barrier spit, and a sink for material scoured from the lengthening inlet. The proposed mechanism for spit growth may be applicable to other locations with low wave energy, small tidal prisms, and low longshore sand transport rates, suggesting that estimates of directions and rates of longshore sand transport based on spit geomorphology and development be scrutinized on a case-by-case basis.

TASK    5)    Description and quantification of sea-level rise throughout the
United States over the past century: Because of our interest in the evolution
and fate of estuarine systems which scale like the small inlets studied during
this contract, a study was done of historical trends in sea-level rise around
the U.S. coastlines over the past century.  Besides altering the size of the
bay drainage system through overwash and landward barrier migration, the rise
of sea level has an important controlling influence on the mean channel depth
within these estuaries.  This controlling depth is an important factor in
numerical model studies of inlet behavior, and subsequent sediment transport.
Rather than examine sea-level change for a single location, changes over the
U.S. shores were calculated using eigenanalysis; the results show spatial
distributions of sea-level change which can be related in a qualitative sense
to estuarine behavior along all U.S. coast' over the past century.  A
scientific paper has resulted from this work, titled 'Eigenanalysis of recent
United States sea levels', by D.G. Aubrey and K.O. Emery (1983).  An abstract
of the paper follows:

Spatial and temporal patterns of recent sea-level rise along the U.S.
coastline have been examined to ascertain rates of rise, and possible causes
for high-frequency fluctuations in sea level.  Eigenanalysis identified several
distinct coastal compartments within each of which sea-level behavior is con-
sistent.  The U.S. east coast has three of these compartments:  one north of
Cape Cod, where sea-level rise increases with distance to the north; one
between Cape Cod and Cape Hatteras where sea-level rise increases to the south;
and the third from Cape Hatteras south to Pensacola, where sea-level rise
decreases to the south.  The western gulf coast represents another compartment
(poorly sampled in this study), where subsidence is partly due to compaction.

The final compartment is along the U.S. west coast, where poor spatial sampling produces a highly spatially variable sea-level record that has some temporal uniformity. Spectral analysis shows a dominant time scale of six years for sea-level variability, with different coastal compartments responding relatively in or out of phase. No evidence for increased rates of sea-level rise over the past ten years was found. This objective statistical technique is a valuable tool for identifying spatial and temporal sea level trends in the United States. It may later prove useful for identifying elusive world-wide trends of sea level, related to glacial melting, glacial rebound, tectonism, and volcanic activity.

TASK     6)    Historical description of tidal inlet and barrier beach behavior over the past three centuries as corroborative data for evaluating the generality of our inlet sediment transport modeling studies: As a preliminary stage to our tidal inlet modeling work, we investigated the long-period (order of 300 years) behavior of a number of tidal inlets to guide us in selecting the most important aspects of inlet migration/barrier beach development, and to suggest important dynamical considerations controlling these major shoreline change episodes. The historical perspective serves as a guide to modeling of natural systems; although not all aspects of system benavior observed in an historical analysis can be mathematically modeled, the historical change provides a means to assure that the problem addressed is a significant one (at least locally).

Two inlets with particularly large-scale changes (Popponesset Inlet and Nauset Inlet) were the subject of technical reports published within WHOI. They describe the historical development and probable causes for these particular patterns of development; these results were then used as data on which modeling efforts were concentrated. Results of these modeling efforts are presented elsewhere in this report.

The first inlet, Popponesset Inlet, Mashpee, Cape Cod, MA, was discussed in a report by Aubrey and Gaines (1982) titled 'Recent evolution of an active barrier beach complex: Popponesset Beach, Cape Cod, Massachusetts'. The abstract of this report follows:

The geomorphic evolution of a small barrier beach on Nantucket Sound was analyzed using historical charts and aerial photographs spanning two centuries. Dramatic changes are associated with the length of the beach and its onshore migration, the geometry of a small island and the location of inlets and breachways. Beach length has changed by about 1.5 km --- first in a growth phase from about 1844 to 1954, and then in an attrition phase from 1955 to the present. Landward migration of the beach has amounted to 55-140 meters since 1938, including both long-term trends and storm displacements, but narrowing of the beach has not been dramatic. Dredging in nearby waters has involved relatively large quantities of sand but neither dredging nor shoreline structures appear responsible for large changes in the subaerial beach. Several lines of evidence suggest longshore drift is also too small to account for the observed changes. A process is proposed, involving exchange of sediment between the inlet channel and the spit, that can account for both growth and attrition of the beach and which is consistent with other characteristics of this area. Certain management implications of the study are outlined.

The second inlet studied, Nauset Inlet, Orleans/Eastham, MA, was the subject of a paper by Speer, Aubrey and Ruder (1982), titled 'Beach changes at Nauset Inlet, Cape Cod, Massachusetts'. A copy of the abstract of this report follows:

A historical study of barrier beach and inlet changes for the Nauset Inlet region, Cape Cod, Massachusetts, was performed to document patterns of beach and inlet change as a preliminary to designing and carrying out field studies of inlet sediment transport. 120 historical charts from 1670 and 125 sets of aerial photographs from 1938 formed the basis for this study. Specific aspects of barrier beach and inlet change addressed include onshore barrier beach movement, longshore tidal inlet migration, and longshore sand bypassing past the inlet. In an effort to correlate forcing events with barrier changes, an exhaustive study of the local storm climate was performed. Detailed treatment of the specific mechanisms responsible for Nauset Inlet migration episodes in a direction opposite the dominant littoral drift are treated in a companion paper by Aubrey, Speer, and Ruder (1982). Documentation of the data base available for the Nauset Area is presented herein as appendices.

TASK    7)    <u>Miscellaneous technical details related to the conduct of nearshore research</u>: As a result of performing this tidal inlet research, several technical topics were addressed which have an impact on many elements of the oceanographic community. These were published in technical reports and scientific papers. The major technical aspects discussed were:

a)    Joining of nearshore electrical cables:  Because of the need to obtain a rapid, low-cost, and reliable connection between electrical cables in the harsh nearshore environment, we carried on some research begun elsewhere

on specific cable joining techniques.  Although expensive, commercially-available techniques can be used in this environment, they are generally too expensive for many projects.  A paper describing low cost cable joining technology was written by Spencer and Aubrey (1981) titled 'Jointing of polyethylene-insulated cable to neoprene jacketed connectors'.  The abstract follows:

Low cost, waterproof, easily implemented jointing of armored electrical cable to neoprene jacketed cable has been required for power/signal cables deployed in the nearshore zone.  The primary difficulty in jointing was associated with bonding to polyethylene insulation within the armored cable. The most troublesome problems encountered were field reliability and deterioration with prolonged storage.  Four methods of jointing with histories of variable performance have been used by the Shore Processes Laboratory (SPL) of Scripps Institution of Oceanography; these techniques were all inexpensive, and readily implemented in the field.  Two methods used encapsulations, one used a heat shrink tubing while another consisted of a mechanical device.

b)   Wave analysis hardware and theory:  Because of the need for obtaining accurate wave directional spectra for the modeling aspects of this study, considerable time was spent in selecting an instrument for this duty, as well as selecting a proper analysis scheme for examining the data.  Specifications for a point directional wave gage for use in the inner shelf were given to Sea Data Corporation (Newton, MA), who constructed a directional wave gage using a precision quartz pressure sensor and a two-axis electromagnetic current meter.  Although similar instruments have been used in the past, this device is one of the first which is readily available to the general oceanographic community with a full range of sampling options.  Aubrey (1981) describes the

-63-

instrument in a technical report; the behavior of the instrument as compared to a number of other shallow water in situ and remote sensors is described in a manuscript by Grosskopf, Aubrey, and Mattie (in press), titled 'Field intercomparison of directional wave sensors'. Abstracts of both papers follow:

i) A directional wave gage consisting of a two-axis electromagnetic current meter and a pressure sensor, developed by Sea Data Corporation, with modifications specified by the author, was successfully deployed during the joint NOAA/U.S. Army Corps of Engineers Coastal Engineering Research Center's Atlantic Remote Sensing Land/Ocean Experiment (ARSLOE) during November, 1980. Data recovery rate was $100^{\circ}/\circ$, and instrument function was verified through comparison with a four-element pressure sensor array at the same location, an X-band imaging radar, _nd with surface meteorological observations charting developing local wave fields. The instrument was proven to be a viable alternative for point measurements of directional wave fields and for estimating the first five fourier coefficients in a directional wave model.

ii) Five measurement strategies (four in situ, one remote) for estimating directional wave spectra were intercompared in a field experiment at Duck, NC in 1981. The systems included two pressure sensor/biaxial current meter combinations (different manufacturers), a triaxial acoustic current meter, an Sxy gage (square array of four pressure sensors), and a shore-based imaging radar. A detailed error analysis suggests sources for differences in estimated wave spectra from the different instruments; in general they intercompare favorably. The major deviation among in situ gages was associated with the triaxial acoustic current meter. Reliance on a "noisy" vertical velocity signal (instead of a direct pressure or sea surface elevation measurement) contributed unacceptable uncertainty in the frequency spectral estimates. The

imaging radar was successful in distinguishing multiple wave trains at the same frequency, which was not possible with the simple spectral estimation analysis applied to in situ data. However, the radar is not useful in providing accurate estimates of spectral density, nor in distinguishing multiple wave trains of different frequencies coming from the same direction. Selection of a measurement strategy for a particular situation depends on the precise data requirements for that application. Although all five tested strategies intercompared well, in practice not all are equally suitable for every application.

c)   Nearshore navigation system:  The modeling and field experiments used to address problems of tidal inlet sediment transport are require accurate bathymetry.  Part of each field experiment was devoted to acquiring bathymetry with accompanying accurate navigation.  To accomplish this, we combined a 200 kHz echo-sounder with a data logger and microwave navigation device to obtain raw bathymetric/position data.  Subsequently we have developed a series of computer software packages to process this data to obtain a fully corrected bathymetric chart.  Shoreline position is normally described by stereo, map-quality vertical aerial photography taken during the time of the experiment.

The echo-sounder used in this study is a Raytheon DE-719C, with the digitizer option and narrow-beam transducer (not really necessary in such shallow water).  Output was generally on an analog recorder, whicn was digitized on a microprocessor based digitizer tablet (Calcomp 9000 series digitizer with an IBM personal computer controlling).  Although the Raytheon digitizer provides digital information for later processing, the bedform size and scales made its use impractical for much of our work.

Navigation was based on a Del Norte Trisponder system, using the model 540 (a micro-processor based system). BCD output from the trisponder was logged on a Sea Data model 1250 data logger, at a user-defined rate (generally in the 0.3-4. hz range).

In the laboratory, navigation and bathymetry were merged, and tidal corrections added from field measurements. The result is a high quality, accurate bathymetric chart of a nearshore region (figure 18). Details of tnis procedure are to be written up in a technical report by S. Gegg, and D. Aubrey.

TOWN COVE

ORLEANS/EASTHAM, MA.

BENCHMARK DESCRIPTION (MASS. COORDINATES - FT.)

1 GOOSE HUMMOCK: X = 1,013,850  Y = 293,290
2 ROCKY POINT: X = 1,016,250  Y = 294,465
3 YACHT CLUB: X = 1,012,813  Y = 290,710

MEAD'S PIER

HOPKINS ISLAND

2 ROCKY POINT

-N-

GOOSE HUMMOCK

1.0
1.5
2.0
2.5
3.0
3.5
4.0
4.5
5.0
5.5

ORLEANS YACHT CLUB

DEPTHS IN METERS
SHORELINE IS APPROXIMATE HIGH WATER MARK
BATHYMETRY FROM 27 AUGUST, 1981
SHORELINE FROM 20 OCTOBER, 1982
VERTICAL DATUM IS MEAN WATER LEVEL FOR
   24-28 AUGUST, 1981

- - - -   APPROXIMATE CHANNEL LIMITS (MAXIMUM CHANNEL
          DEPTH APPROXIMATELY 2 METERS). DEPTH OUTSIDE
          CHANNEL IS GENERALLY LESS THAN 2 METERS.

-..:..-   APPROXIMATE EEL GRASS LIMITS

   +      DEEPEST POINT - 6.0M

0   100  200  300  400  500
        (METERS)

BY: D AUBREY and S. GEGG     MARCH, 1983
DRAWN BY: V. FRY

Figure 18.  Bathymetric map of Town Cove and feeder channels, based on surveys from
            1981, using a micro-wave navigation device and a high-resolution echo-
            sounder, processed through computer software developed as part of this
            study.

## REFERENCES

Aubrey, D.G., 1981. Field evaluation of Sea Data directional wave gage (Model 635-9). Woods Hole Oceanographic Institution Technical Report, WHOI-81-28, 52 pp.

Aubrey, D.G., P.E. Speer and E. Ruder. Updrift migration of tidal inlets: a natural response to wave, tide and storm forcing. Submitted to G.S.A.

Aubrey, D.G. and A.G. Gaines, 1982. Recent evolution of an active barrier beach complex: Popponesset Beach, Cape Cod, Massachusetts, Woods Hole Oceanographic Institution Technical Report, No. 82-3, 77 pp.

Aubrey, D.G. and A.G. Gaines, 1982. Rapid formation and degradation of barrier spits in areas with low rates of littoral drift. Marine Geology, v. 49, p. 257-278.

Aubrey, D.G. and K.O. Emery, 1983. Eigenanalysis of recent United States sea levels. Continental Shelf Research, v. 2, p. 21-33.

Aubrey, D.G. and P.E. Speer, 1982. Propagation of tidal disturbances through a shallow estuarine embayment. Abstract, AGU/ASLO Joint Meeting, San Antonio, Texas.

Aubrey, D.G. and P.E. Speer, in prep., Non-linear tidal distortion in a shallow estuarine embayment.

Boon, J.D. III and K.P. Kiley, 1978. Harmonic analysis and tidal prediction by the method of least squares. Spec. Report No. 186, Virginia Institute of Marine Science, Gloucester Pt., VA, 49 pp.

Boon, J.D. and R.J. Byrne, 1981. On basin hypsometry and the morphodynamic response of coastal inlet systems. Marine Geology, v. 40, p. 27-48.

Bridge, J.S., 1977. Flow, bed topography, grain size and sedimentary structure in bends: a three dimensional model: Earth Surface Processes, v. 1, p. 303-336.

Byrne, R.J., J.T. DeAlteris and J.P. Sovich, 1977. Recent history and response characteristics of Wachapreague Inlet, VA. Final report to ONR Geography Programs, VIMS, Gloucester Pt., VA, 127 pp. and Appen.

Chen, R.N. and L.A. Hembree, 1977. Numerical Simulation of Hydrodynamics (TRACOR), Appen. 3, G.I.T.I. Report 6. U.S. Army Coastal Engr'g Research Center, Ft. Belvoir, VA, 254 pp.

Dennis, R.E. and E.E. Long, 1971. "A Users guide to a Computer for Harmonic Analysis of Data at Tidal Frequencies," NOAA Technical Report NOS-41, July.

Dietrich, W.E., J.D. Smith and T. Dunne, 1979. Flow and sediment transport in a sand bedded meander. Jour. Geology, v. 87, p. 305-315.

Dietrich, W.E., 1982. Flow, boundary shear stress, and sediment transport in a river meander, Ph.D. dissertation, Department of Geological Sciences, University of Washington, 261 p.

Dronkers, J.J., 1964. Tidal Computations in Rivers and Coastal Waters. North-Holland Publishing Company, Amsterdam, The Netherlands, 516 pp.

Engelund, F., 1974. Flow and bed topography in channel bends: Jour. Hydraulic Div., Amer. Soc. Civ. Engineers, v. 100, No. HY11, p. 1631.

Finley, R.J., 1976. Hydraulics and Dynamics of North Inlet, South Carolina, 1974-75. G.I.T.I. Report 10, U.S. Army Coastal Engr'g Research Center, Ft. Belvoir, VA, 188 pp.

Grant, W.D. and O.S. Madsen, 1982. Moveable bed roughness in unsteady oscillatory flow. Jour. Geophys. Res., v. 87, p. 469-481.

Grosskopf, W.G., D.G. Aubrey and M.G. Mattie. Field intercomparison of nearshore directional wave sensors, in press, IEEE.

Hooke, R. LeB., 1975. Distribution of sediment transport and shear stress in a meander bend, Jour. of Geology, v. 83, p. 543-565.

Ianniello, J.P., 1977. Tidally induced residual currents in estuaries of constant breadth and depth. Journal of Marine Research, v. 35, p. 755-786.

King, C.A.M., 1972. Beaches and Coasts, second edition, Edward Arnold, London, England, 570 pp.

Kreiss, H., 1957. Some remarks about nonlinear oscillations in tidal channels. Tellus, v.9, p. 53-63.

LeBlond, P.H., 1978. On tidal propagation in shallow rivers. Journal Geophys. Res., v. 83, p. 4717-4721.

Leschziner, M.A., and W. Rodi, 1979. Calculation of strongly curved open channel flow. Jour. Hydr. Div., ASCE, v. 105, No. HY10, p. 1297-1314.

Longuet-Higgins, M.S., 1969. On the transport of mass by time-varying ocean currents. Deep-Sea Research, v. 16, p. 431-447.

Masch, F.D., R.J. Brandes and J.D. Reagan, 1977. Numerical simulation of hydrodynamics (WRE). Appen. 2, v. 1, G.I.T.I. Report 6, U.S. Army Coastal Engr'g Center, Ft. Belvoir, VA, 123 pp. and Appen.

Munk, W.H. and D.E. Cartwright, 1966. Tidal spectroscopy and prediction. Phil. Trans. of Royal Soc. of London, v. 259, p. 533-581.

Nouh, M.A. and R.D. Townsend, 1979. Shear-stress distribution in stable channel bends. Jour. Hydr. Div., ASCE, v. 105, No. HY10, p. 1233-1245.

Nummedal, D. and S.M. Humphries, 1978. Hydraulics and dynamics of North Inlet, 1975-76. G.I.T.I. Report 16, U.S. Army Coastal Engr'g Center, Ft. Belvoir, VA, 214 p.

Orlanski, I., 1976. A simple boundary condition for unbounded hyperbolic flows. Journal of Computational Physics, v. 21, p. 251-269.

Pingree, R.D. and L. Maddock, 1978. The $M_4$ tide in the English Channel derived from a non-linear numerical model of the $M_2$ tide. Deep-Sea Research, v. 26, p. 53-68.

Pingree, R.D. and D.K. Griffiths, 1979. Sand transport paths around the British Isles resulting from $M_2$ and $M_4$ tidal interactions. J. Mar. Bio. Ass. U.K., v. 59, p. 497-513.

Prandle, D., 1980. Modeling of tidal barrier schemes: an analysis of the open-boundary problem by reference to AC circuit theory, Est. and Coast. Mar. Sci., v. 2, 53-71.

Reid, R.O. and B.R. Bodine, 1968. Numerical model for storm surges in Galveston Bay. American Society of Civil Engineers, Journal of Waterways and Harbors Division, No. WWI, p. 33-57.

Reid, R.O. A.C. Vastano and T.J. Reid, 1977. Development of SURGE II program with application to the Sabine-Calcasieu area for Hurricane Carla and design hurricanes. Technical Paper No. 77-13, U.S. Army Coastal Engr'g Research Center, Ft. Belvoir, VA, 218 pp.

Robinson, I.S., 1980. Tides in the Bristol Channel - an analytical wedge model with friction. Geophys. Journ. Roy. Astr. Soc., v. 62, p. 77-95.

Schureman, P., 1971. "Manual of Harmonic Analysis and Prediction of Tides," U.S. Dept. of Commerce, Coast and Geodetic Survey, Special Publ. No. 98, Revised 1940 Edition, Published 1971.

Seelig, W., D.L. Harris and B.E. Herchenroder, 1976. A spatially integrated numerical model of inlet hydraulics. G.I.T.I. Report 14, U.S. Army Coastal Engr'g Research Center, Ft. Belvoir, VA, 101 pp.

Seelig, W. and R.M. Sorensen, 1978. Numerical model investigations of selected tidal inlet-bay system characteristics. In Proceedings of the 16th Coastal Engineering Conference, A.S.C.E., Hamburg, W. Germ., p. 1302-1319.

Smith, J.D. and S.R. McLean, in prep. A model for meandering streams.

Speer, P.E., D.G. Aubrey and E. Ruder, 1982. Beach changes at Nauset Inlet, Cape Cod, Massachusetts, 1670-1981. Woods Hole Oceanographic Institution Technical Report, No. 82-40, 92 pp.

Spencer, W.D. and D.G. Aubrey, 1981. Jointing of polyethylene-insulated cable to neoprene jacketed connectors. Oceans, IEEE, p. 180-185.

Uncles, R.J. and M.B. Jordan, 1980. A one-dimensional representation of residual currents in the Severn Estuary and associated observations. Estuarine and Coastal Marine Science, v. 10, p. 39-60.

Uncles, R.J., 1981. A note on tidal asymmetry in the Severn Estuary. Estuarine, Coastal and Shelf Science, v. 13, p. 419-432.

Van de Kreeke, J. 1976. Increasing the mean current in coastal channels. Journal of the Waterways, Harbors and Coastal Engineering Division, A.S.C.E., v. 102, No. WW2, p. 223-234.

Van de Kreeke, J. and R.G. Dean, 1975. Tide-induced mass transport in lagoons. Journal of the Waterways, Harbors and Coastal Engineering Division, A.S.C.E., v. 101, No. WW4, p. 393-403.

Van de Kreeke, J., J.H. Carpenter and D.S. McKeehan, 1977. Water motions in a closed-end residential canal. Journal of the Waterways, Port, Coastal and Ocean Division, A.S.C.E., v. 103, No. WW1, p. 161-166.

Van de Kreeke, J. and S.S. Chiu, 1980. Tide-induced residual flow. In Mathematical Modelling of Estuarine Physics, J. Sundermann and K.-P. Holz (eds.), Springer-Verlag, Berlin, p. 133-144.

Wang, J.D., 1980. Analysis of tide and current meter data for model verification. In Mathematical Modelling of Estuarine Physics, J. Sundermann and K.-P. Holz (eds.), Springer-Verlag, Berlin, p. 156-170.

Watson, R.L. and E.W. Behrens, 1976. Hydraulics and dynamics of New Corpus
Christi Pass, Texas: A case history, 1972-1975. G.I.T.I. Report 9, U.S.
Army Coastal Engr'g Research Center, Ft. Belvoir, VA.

Wurtele, M.G., J.P. Paegle and A. Selecki, 1971. The use of open boundary
conditions with the storm-surge equations. Monthly Weather Review, v. 99,
No. 6, p. 537-544.

Yen, C., and Yen, B., 1971. Water surface configuration in channel bends,
Jour. Hydraulics Division, Amer. Soc. Civ. Engineers, v. 97, No. HY2, p.
303-321.

## PUBLICATIONS

The following publications were supported at least in part by the U.S. Army Research Office:

## SCIENTIFIC ARTICLES

Aubrey, D.G. and A.G. Gaines, 1982. Rapid formation and degradation of barrier spits in areas with low rates of littoral drift. Marine Geology, v. 49, p. 257-278.

Aubrey, D.G., P.E. Speer and E. Ruder. Updrift migration of tidal inlets: a natural response to wave, tide and storm forcing. Submitted to G.S.A.

Grosskopf, W.G., D.G. Aubrey and M.G. Mattie. Field intercomparison of nearshore directional wave sensors, in press, IEEE.

Aubrey, D.G. and K.O. Emery. Eigenanalysis of recent United States sea levels. Continental Shelf Research, in press.

## TECHNICAL REPORTS

Aubrey, D.G., 1981. Field evaluation of Sea Data directional wave gage (Model 635-9). Woods Hole Oceanographic Institution Technical Report, WHOI-81-28, 52 pp.

Spencer, W.D. and D.G. Aubrey, 1981. Jointing of polyethylene-insulated cable to neoprene jacketed connectors. Oceans, IEEE, p. 180-185.

Aubrey, D.G. and A.G. Gaines, 1982. Recent evolution of an active barrier beach complex: Popponesset Beach, Cape Cod, Massachusetts, Woods Hole Oceanographic Institution Technical Report, No. 82-3, 77 pp.

Speer, P.E., D.G. Aubrey and E. Ruder, 1982. Beach changes at Nauset Inlet, Cape Cod, Massachusetts, 1670-1981. Woods Hole Oceanographic Institution Technical Report, No. 82-40, 92 pp.

## SCIENTIFIC PRESENTATIONS

The following talks presented at major scientific meetings were based at least in part on research performed under the auspices of the U.S. Army Research Office. In addition, approximately a dozen presentations covering this material have been made at universities throughout the world.

Aubrey, D.G. and D.C. Twichell, 1980. Holocene sedimentation in a Pleistocene glacial depression, Cape Cod Massachusetts, Abstract, Northeastern Section GSA, Philadelphia, Pennsylvania.

Aubrey, D.G. and P.E. Speer, 1981. Tidal behavior through a tidal inlet. Spring Meeting, AGU,, Baltimore, Maryland.

Aubrey, D.G. and P.E. Speer, 1982. Propagation of tidal disturbances through a shallow estuarine embayment. AGU/ASLU Meeting, San Antonio, TX.

Grosskopf, W.G., D.G. Aubrey, M.G. Mattie, M. Mathiesen, and R.J. Seymour, 1982. Field intercomparison of nearshore directional wave sensors. Oceans '82, Washington, D.C.

Speer, P.E., D.G. Aubrey, and E. Ruder, 1983. Updrift migration of tidal inlets: a natural response to wave, tide, and storm forcing. N.E. Regional GSA meeting, NY.

## SCIENTIFIC PERSONNEL

The principal investigator on this project has been Dr. D.G. Aubrey. Other Woods Hole researchers have helped out in a variety of elements of this research, in terms of manpower, instrumentation, and as a source for scientific discussion. Chief among these have been Dr.'s A.J. Williams III and William D. Grant of the Ocean Engineering Department.

A graduate student, P.E. Speer, has been partly supported on Army Research Office grants for his dissertation research. Mr. Speer's dissertation is focused on theoretical and field analysis of tidal distortion in shallow estuaries. He is expected to finish this work by the end of 1983.

## TWO-DIMENSIONAL EQUATIONS:

The two-dimensional depth-averaged equations are presented below with non-linear terms analogous to the one-dimensional case underlined (e.g., Dronkers, 1964).

$$\frac{\partial \zeta}{\partial t} + \frac{\partial}{\partial x} \underbrace{(h+\zeta)\,\bar{u}}_{I} + \frac{\partial}{\partial y} \underbrace{(h+\zeta)\,\bar{v}}_{I} = 0 \qquad \text{Continuity}$$

$$\frac{\partial \bar{u}}{\partial t} + \underbrace{\bar{u}\frac{\partial \bar{u}}{\partial x} + \bar{v}\frac{\partial \bar{u}}{\partial y}}_{II} = -g\frac{\partial \zeta}{\partial x} - \underbrace{\frac{C_D\, q\, \bar{u}}{(h+\zeta)}}_{III} \qquad X - \text{Momentum}$$

$$\frac{\partial \bar{v}}{\partial t} + \underbrace{\bar{u}\frac{\partial \bar{v}}{\partial x} + \bar{v}\frac{\partial \bar{v}}{\partial y}}_{II} = -g\frac{\partial \zeta}{\partial y} - \underbrace{\frac{C_D\, q\, \bar{v}}{(h+\zeta)}}_{III} \qquad y - \text{Momentum}$$

where

$$\bar{u} = \frac{1}{(h+\zeta)} \int_{-h}^{\zeta} u\,dz$$

$$\bar{v} = \frac{1}{(h+\zeta)} \int_{-h}^{\zeta} v\,dz$$

$h$ = undisturbed water depth

$\zeta$ = tidal elevation perturbation

$q = (\bar{u}^2 + \bar{v}^2)^{\frac{1}{2}}$

$C_D$ = drag coefficient

The underlined non-linear terms can be described as follows:

I )    divergence of volume flux associated with region between undisturbed water depth and tidal free surface elevation.

II )    advection of momentum

III)    quadratic friction.

The momentum equations neglect Coriolis terms (linear) and horizontal diffusion of momentum (generally taken as linear).

## RESIDUAL CURRENTS--DEFINITIONS

This section defines residual currents which result from a time-average of non-linear terms in the equations of motion. Consider the instantaneous depth-integrated flux in a rectangular channel:

$$q = (h + \zeta)\bar{u} \tag{1}$$

where

$$\bar{u} = \frac{1}{(h+\zeta)} \int_{-h}^{\zeta} u(z)\,dz$$

We may consider the depth-mean flow as consisting of a time-averaged and periodic component

$$\bar{u} = u_E + u_p$$

$$u_E = \frac{1}{T} \int_0^T \bar{u}\,dt \qquad\qquad T = \text{tidal cycle}$$

$$u_p = \text{periodic mean velocity component}$$

similarly with $\zeta$,

$$\zeta = \zeta_E + \zeta_p$$

$$\zeta_E = \frac{1}{T} \int_0^T \zeta\,dt$$

We take a time average of (1) over a tidal cycle:

$$\langle q \rangle = h \cdot u_E + \langle \zeta_p \cdot u_p \rangle$$

Dividing by h yields the Lagrangian mean velocity,

$$\frac{\langle q \rangle}{h} = u_E + \frac{\langle u_p \zeta_p \rangle}{h}$$

We find that the Lagrangian mean velocity consists of the Eulerian residual flow, $u_E$, and the stokes drift, $\frac{\langle \zeta_p u_p \rangle}{h}$, resulting from non-zero correlations between sea surface elevation and velocity. Defining $\frac{\langle q \rangle}{h} = u_L$ we may define a flushing time for a coastal channel of length L:

$$T_f = \frac{L}{u_L}$$

# APPENDIX II

Following is a series of harmonic analyses for the tide gage stations discussed under Task 1 and summarized in Table 4. Locations are given in Figures 2 and 3. Dominant tidal constituents are listed in a table preceding each figure. ζ is the phase referenced to the beginning of the time series. G is the equivalent Greenwich equilibrium phase for the constituent. The variances for the observed and residual signal are listed (note that forecast series have no residual variance, by definition).

Confidence intervals for the constituent variances, amplitudes and phases are contained in a companion publication in preparation by Aubrey, Boon and Speer.

STATION:  OCEAN GAGE          LATITUDE:  41.82°N          LONGITUDE:  69.90°W

DATE:  18/10/82 - 16/11/82                    (forecast)

| CONSTITUENT | AMPLITUDE (M) | ς (deg.) | G (deg.) |
|---|---|---|---|
| $M_2$ | 1.027 | 56 | 98 |
| $S_2$ | .129 | 77 | 146 |
| $N_2$ | .197 | 149 | 75 |
| $K_1$ | .149 | 70 | 212 |
| $M_4$ | .005 | 199 | 283 |
| $O_1$ | .115 | 277 | 180 |
| $M_6$ | .004 | 80 | 207 |
| NU2 | .039 | 302 | 75 |
| MU2 | .025 | 32 | 50 |
| 2N2 | .027 | 236 | 46 |
| M1 | .008 | 169 | 196 |
| Q1 | .022 | 16 | 165 |
| P1 | .049 | 292 | 210 |
| L2 | .029 | 145 | 124 |
| K2 | .035 | 45 | 150 |

Recorded variance ($M^2$)          $5.78 \times 10^{-1}$

Residual variance ($M^2$)          ------------

NAUSET INLET TIDES
OCEAN TIDE GAGE
10/82–11/82

M4/M2 = 0.0049
M6/M2 = 0.0039
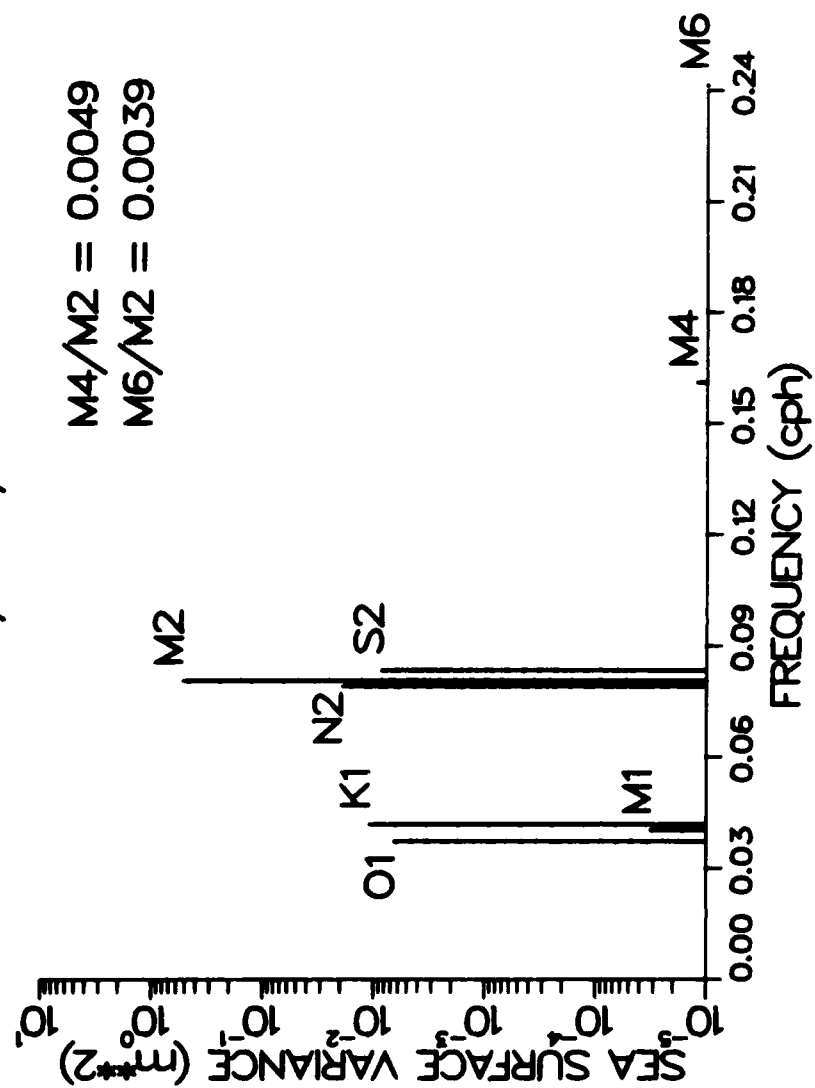
STATION: MIDDLE CHANNEL   LATITUDE: 41.81°N        LONGITUDE: 69.95°W

EAST

DATE:  18/10/82 - 16/11/82

| CONSTITUENT | AMPLITUDE (M) | $\zeta$ (deg.) | G (deg.) |
|---|---|---|---|
| $M_2$ | .661 | 79 | 121 |
| $S_2$ | .068 | 106 | 175 |
| $N_2$ | .082 | 153 | 79 |
| $K_1$ | .101 | 100 | 242 |
| $M_4$ | .052 | 93 | 177 |
| $0_1$ | .080 | 318 | 222 |
| $M_6$ | .021 | 302 | 68 |
| NU2 | .025 | 323 | 96 |
| MU2 | .016 | 50 | 67 |
| 2N2 | .017 | 253 | 63 |
| M1 | .006 | 205 | 232 |
| Q1 | .015 | 64 | 212 |
| P1 | .033 | 323 | 241 |
| L2 | .019 | 171 | 150 |
| K2 | .018 | 74 | 179 |

Recorded variance ($M^2$)     $2.45 \times 10^{-1}$

Residual variance ($M^2$)     $1.05 \times 10^{-2}$

NAUSET INLET TIDES
MIDDLE CHANNEL EAST TIDE GAGE
10/82–11/82

M4/M2 = 0.0787
M6/M2 = 0.0318
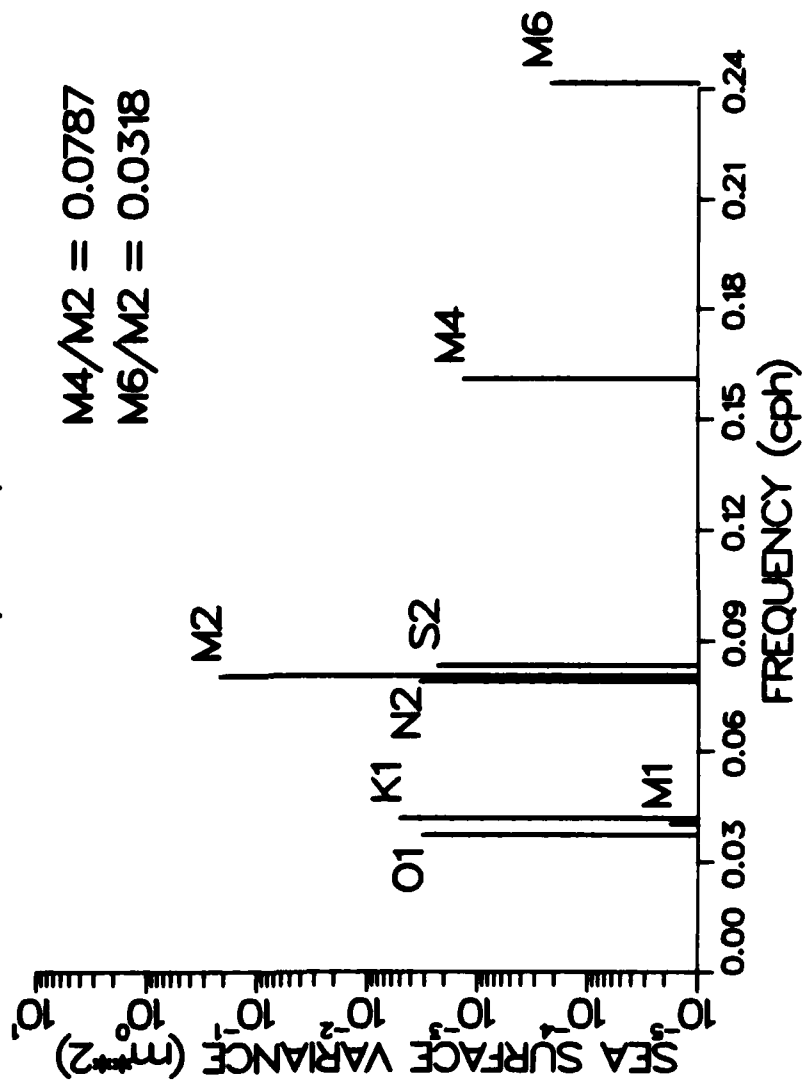
STATION: MIDDLE CHANNEL   LATITUDE: 41.81°N        LONGITUDE: 69.95°W
              WEST

DATE: 18/10/82 - 16/11/82


| CONSTITUENT | AMPLITUDE (M) | $\zeta$ (deg.) | G (deg.) |
|---|---|---|---|
| $M_2$ | .588 | 94 | 136 |
| $S_2$ | .083 | 107 | 176 |
| $N_2$ | .097 | 190 | 116 |
| $K_1$ | .092 | 103 | 245 |
| $M_4$ | .069 | 125 | 209 |
| $O_1$ | .076 | 336 | 240 |
| $M_6$ | .019 | 328 | 95 |
| NU2 | .022 | 345 | 118 |
| MU2 | .014 | 79 | 97 |
| 2N2 | .015 | 284 | 94 |
| M1 | .005 | 215 | 243 |
| Q1 | .015 | 89 | 237 |
| P1 | .031 | 327 | 245 |
| L2 | .016 | 179 | 158 |
| K2 | .023 | 75 | 179 |

Recorded variance ($M^2$)    $2.04 \times 10^{-1}$

Residual variance ($M^2$)    $1.35 \times 10^{-2}$

NAUSET INLET TIDES
MIDDLE CHANNEL WEST TIDE GAGE
10/82–11/82

M4/M2 = 0.1173
M6/M2 = 0.0323
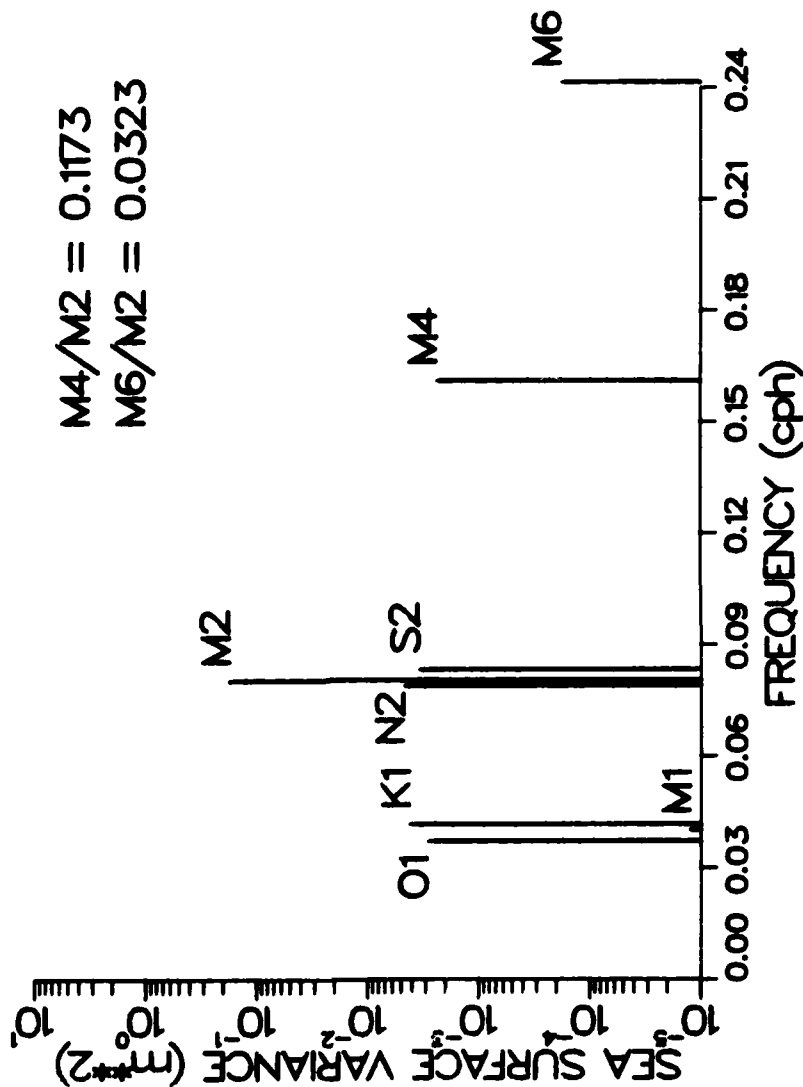
STATION: NAUSET HEIGHTS   LATITUDE: 41.80°N      LONGITUDE: 69.94°W

DATE:  18/10/82 - 16/11/82

| CONSTITUENT | AMPLITUDE (M) | $\zeta$ (deg.) | G (deg.) |
|---|---|---|---|
| $M_2$ | .601 | 93 | 135 |
| $S_2$ | .87 | 107 | 176 |
| $N_2$ | .102 | 189 | 116 |
| $K_1$ | .095 | 102 | 245 |
| $M_4$ | .073 | 336 | 240 |
| $O_1$ | .077 | 336 | 240 |
| $M_6$ | .013 | 355 | 122 |
| NU2 | .023 | 343 | 116 |
| MU2 | .014 | 77 | 94 |
| 2N2 | .016 | 238 | 91 |
| M1 | .005 | 215 | 242 |
| Q1 | .015 | 90 | 238 |
| P1 | .031 | 327 | 244 |
| L2 | .017 | 178 | 157 |
| K2 | .024 | 74 | 179 |

Recorded variance ($M^2$)     $2.14 \times 10^{-1}$

Residual variance ($M^2$)     $1.41 \times 10^{-2}$

NAUSET INLET TIDES
NAUSET HEIGHTS TIDE GAGE
10/82–11/82
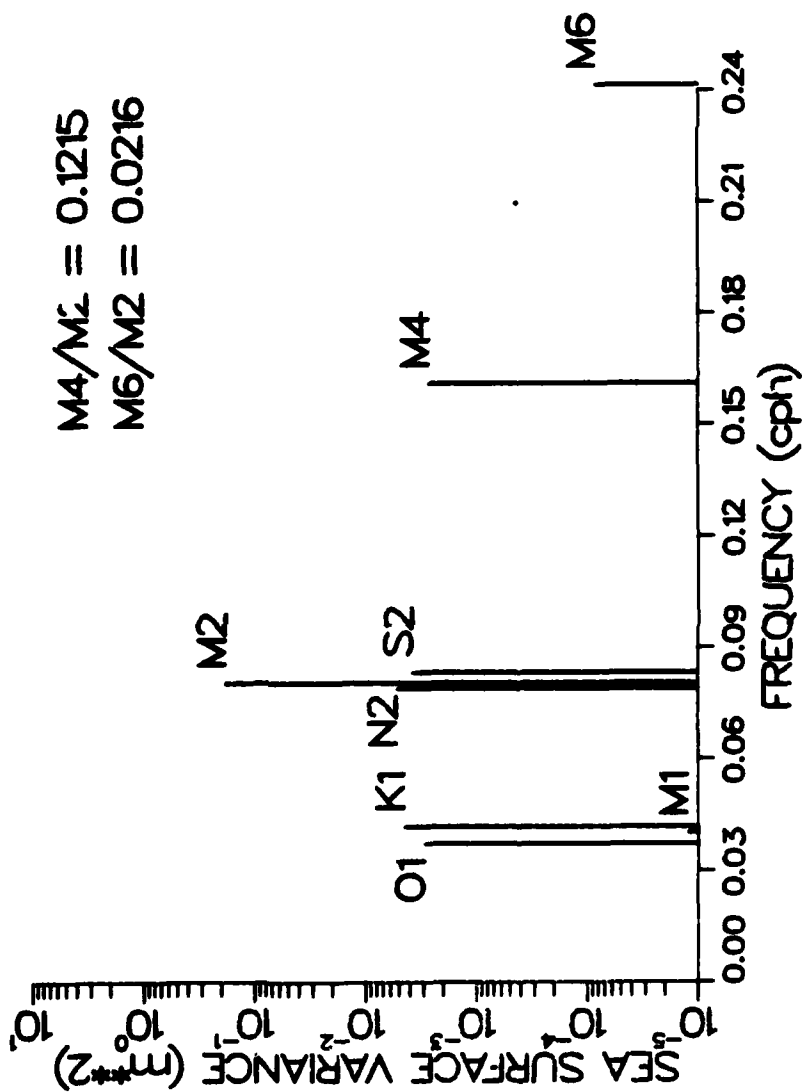
M4/M2 = 0.1215
M6/M2 = 0.0216

STATION: SNOW POINT     LATITUDE: 41.81°N     LONGITUDE: 69.96°W

DATE: 18/10/82 - 16/11/82

| CONSTITUENT | AMPLITUDE (M) | $\zeta$ (deg.) | G (deg.) |
|---|---|---|---|
| $M_2$ | .538 | 105 | 147 |
| $S_2$ | .078 | 116 | 185 |
| $N_2$ | .090 | 202 | 128 |
| $K_1$ | .090 | 109 | 252 |
| $M_4$ | .080 | 149 | 233 |
| $O_1$ | .078 | 343 | 247 |
| $M_6$ | .010 | 335 | 102 |
| NU2 | .020 | 357 | 130 |
| MU2 | .013 | 92 | 110 |
| 2N2 | .014 | 297 | 107 |
| M1 | .006 | 222 | 249 |
| Q1 | .015 | 96 | 244 |
| P1 | .030 | 334 | 251 |
| L2 | .015 | 188 | 168 |
| K2 | .021 | 83 | 188 |

Recorded variance ($M^2$)     $1.75 \times 10^{-1}$

Residual variance ($M^2$)     $1.34 \times 10^{-2}$

NAUSET INLET TIDES
SNOW POINT TIDE GAGE
10/82–11/82

M4/M2 = 0.1487
M6/M2 = 0.0186
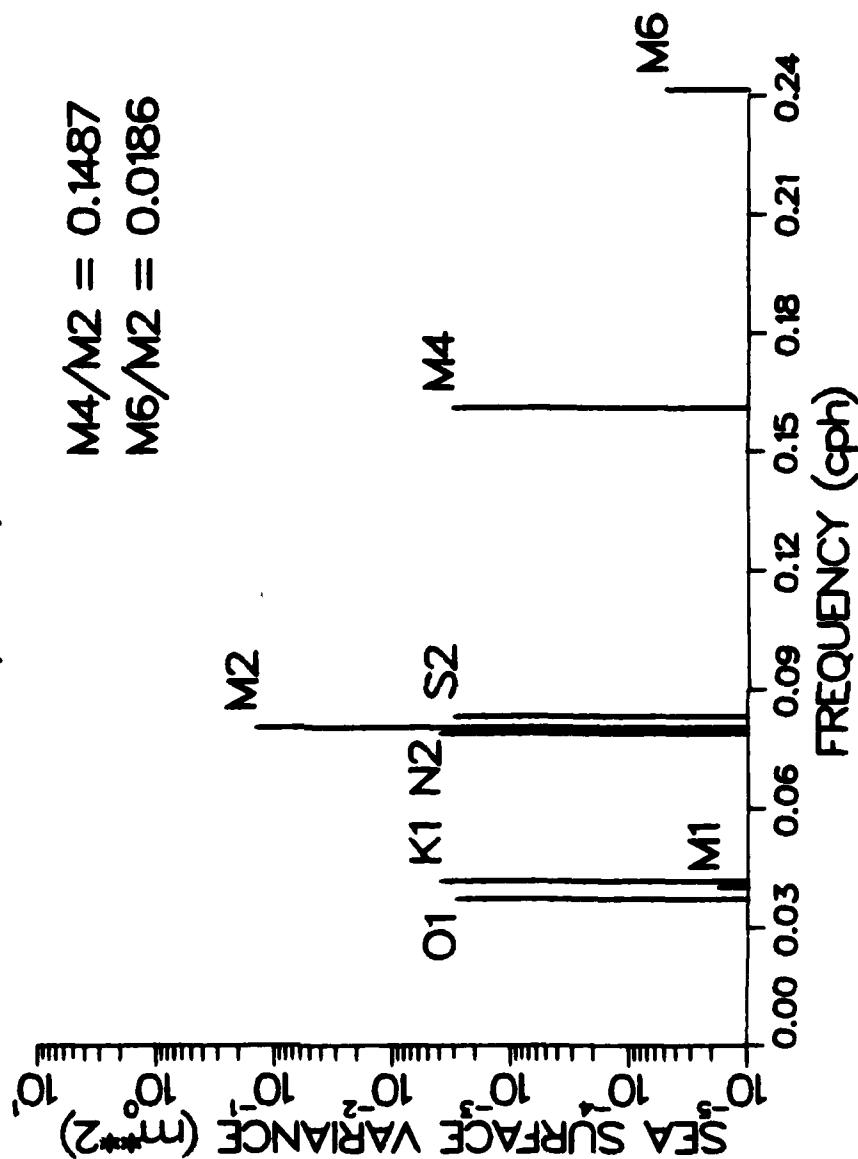
STATION: GOOSE HUMMOCK    LATITUDE: 41.80°N    LONGITUDE: 69.99°W

DATE: 18/10/82 - 16/11/82                 (forecast)

| CONSTITUENT | AMPLITUDE (M) | $\zeta$ (deg.) | G (deg.) |
|---|---|---|---|
| $M_2$ | .551 | 106 | 148 |
| $S_2$ | .054 | 143 | 212 |
| $N_2$ | .097 | 178 | 104 |
| $K_1$ | .091 | 120 | 262 |
| $M_4$ | .112 | 148 | 232 |
| $O_1$ | .093 | 336 | 239 |
| $M_6$ | .015 | 208 | 335 |
| NU2 | .019 | 345 | 118 |
| MU2 | .012 | 66 | 83 |
| 2N2 | .013 | 268 | 79 |
| M1 | .007 | 224 | 251 |
| Q1 | .018 | 80 | 228 |
| P1 | .030 | 343 | 261 |
| L2 | .014 | 203 | 182 |
| K2 | .015 | 113 | 217 |

Recorded variance ($M^2$)        $1.54 \times 10^{-1}$

Residual variance ($M^2$)        -------------

NAUSET INLET TIDES
GOOSE HUMMOCK TIDE GAGE
10/82-11/82

M4/M2 = 0.2192
M6/M2 = 0.0294
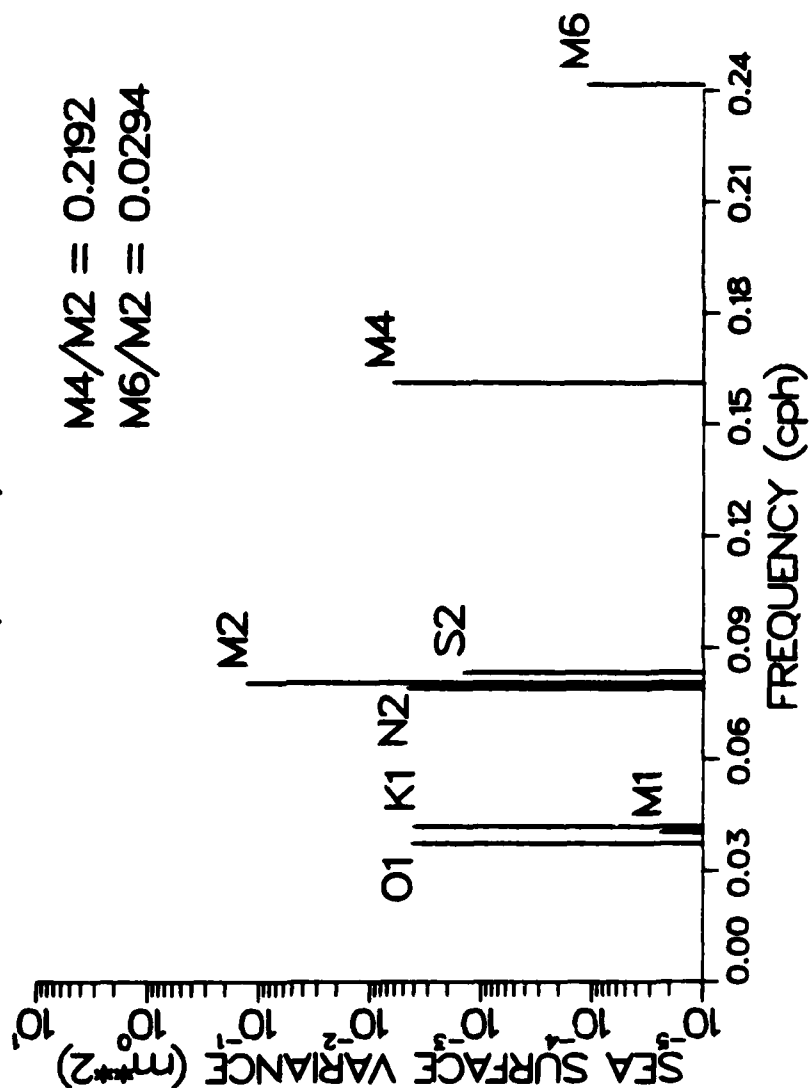
STATION: NORTH CHANNEL    LATITUDE: 41.82°N        LONGITUDE: 69.95°W

DATE:  18/10/82 - 16/11/82                (forecast)

| CONSTITUENT | AMPLITUDE (M) | $\zeta$ (deg.) | G (deg.) |
|---|---|---|---|
| $M_2$ | .441 | 99 | 141 |
| $S_2$ | .063 | 129 | 198 |
| $N_2$ | .102 | 212 | 138 |
| $K_1$ | .073 | 127 | 270 |
| $M_4$ | .083 | 135 | 219 |
| $O_1$ | .072 | 330 | 234 |
| $M_6$ | .002 | 168 | 295 |
| NU2 | .017 | 341 | 114 |
| MU2 | .011 | 66 | 84 |
| 2N2 | .011 | 269 | 80 |
| M1 | .005 | 225 | 252 |
| Q1 | .014 | 68 | 216 |
| P1 | .024 | 350 | 267 |
| L2 | .012 | 192 | 171 |
| K2 | .017 | 98 | 202 |

Recorded variance ($M^2$)        $1.13 \times 10^{-1}$

Residual variance ($M^2$)        ------------

NAUSET INLET TIDES
NORTH CHANNEL TIDE GAGE
10/82–11/82

M4/M2 = 0.1882
M6/M2 = 0.0045
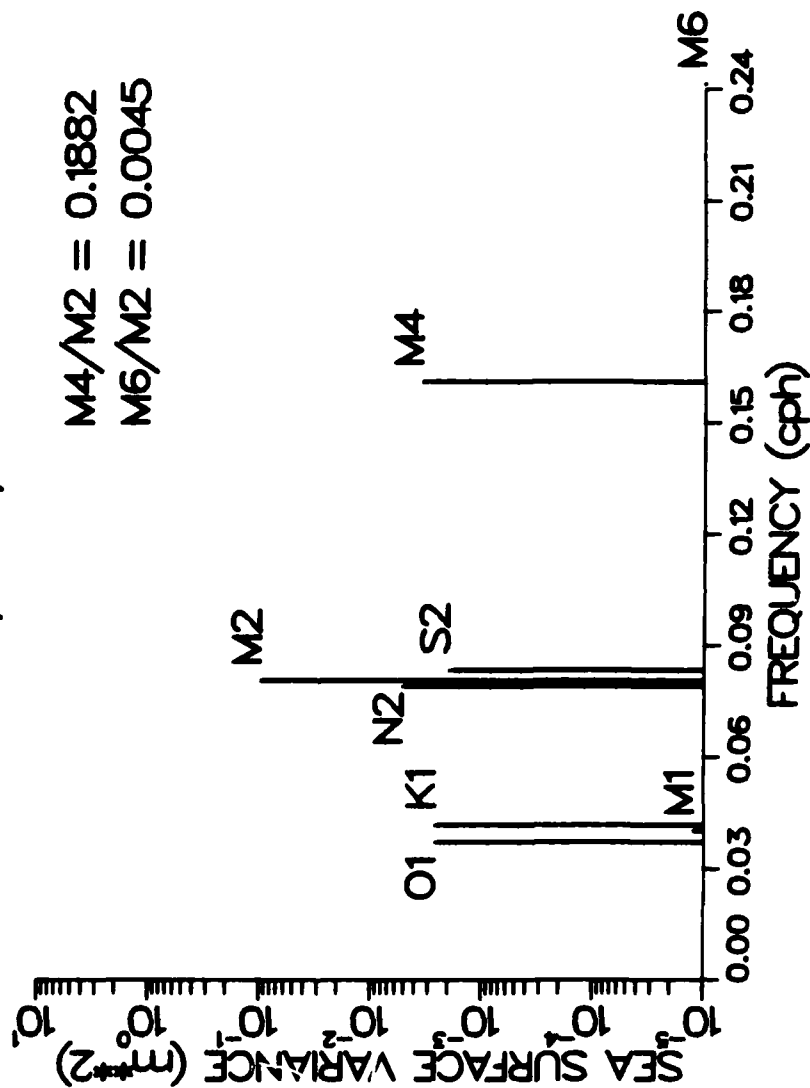
STATION: NAUSET BAY     LATITUDE: 41.83°N     LONGITUDE: 69.96°W

DATE: 18/10/82 - 16/11/82

| CONSTITUENT | AMPLITUDE (M) | $\zeta$ (deg.) | G (deg.) |
|---|---|---|---|
| $M_2$ | .410 | 275 | 317 |
| $S_2$ | .064 | 279 | 348 |
| $N_2$ | .074 | 2 | 288 |
| $K_1$ | .084 | 196 | 338 |
| $M_4$ | .109 | 128 | 212 |
| $O_1$ | .084 | 66 | 330 |
| $M_6$ | .017 | 350 | 117 |
| NU2 | .016 | 170 | 303 |
| MU2 | .010 | 269 | 287 |
| 2N2 | .011 | 114 | 285 |
| M1 | .006 | 307 | 334 |
| Q1 | .016 | 177 | 325 |
| P1 | .028 | 60 | 338 |
| L2 | .011 | 355 | 334 |
| K2 | .017 | 246 | 350 |

Recorded variance $(M^2)$     $1.18 \times 10^{-1}$
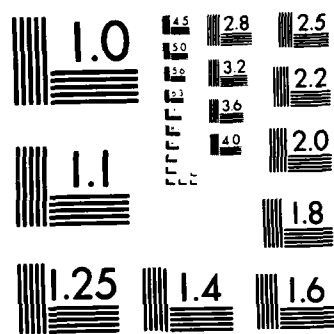
Residual variance $(M^2)$     $1.63 \times 10^{-2}$

END

FILMED

MICROCOPY RESOLUTION TEST CHART

NATIONAL BUREAU OF STANDARDS-1963-A

NAUSET INLET TIDES
NAUSET BAY TIDE GAGE
10/82–11/82

M4/M2 = 0.2659
M6/M2 = 0.0415

STATION: MIDDLE CHANNEL   LATITUDE: 41.81°N       LONGITUDE: 69.96°W

EAST

DATE:   23/9/82 - 22/10/82

| CONSTITUENT | AMPLITUDE (M) | $\zeta$ (deg.) | G (deg.) |
|---|---|---|---|
| $M_2$ | .665 | 179 | 128 |
| $S_2$ | .078 | 80 | 167 |
| $N_2$ | .101 | 302 | 102 |
| $K_1$ | .095 | 113 | 239 |
| $M_4$ | .052 | 294 | 192 |
| $O_1$ | .085 | 43 | 229 |
| $M_6$ | .020 | 244 | 91 |
| NU2 | .025 | 147 | 110 |
| MU2 | .016 | 276 | 89 |
| 2N2 | .017 | 76 | 86 |
| M1 | .006 | 259 | 234 |
| Q1 | .016 | 187 | 224 |
| P1 | .032 | 287 | 239 |
| L2 | .019 | 231 | 149 |
| K2 | .021 | 97 | 170 |

Recorded variance ($M^2$)     $2.76 \times 10^{-1}$

Residual variance ($M^2$)     $3.72 \times 10^{-2}$

NAUSET INLET TIDES
MIDDLE CHANNEL EAST TIDE GAGE
23/9/82–22/10/82

M4/M2 = 0.0782
M6/M2 = 0.0301

M2

S2

K1 N2

O1

M1

M4

M6

SEA SURFACE VARIANCE (m**2)

$10^1$
$10^0$
$10^{-1}$
$10^{-2}$
$10^{-3}$
$10^{-4}$
$10^{-5}$

0.00  0.03  0.06  0.09  0.12  0.15  0.18  0.21  0.24

FREQUENCY (cph)
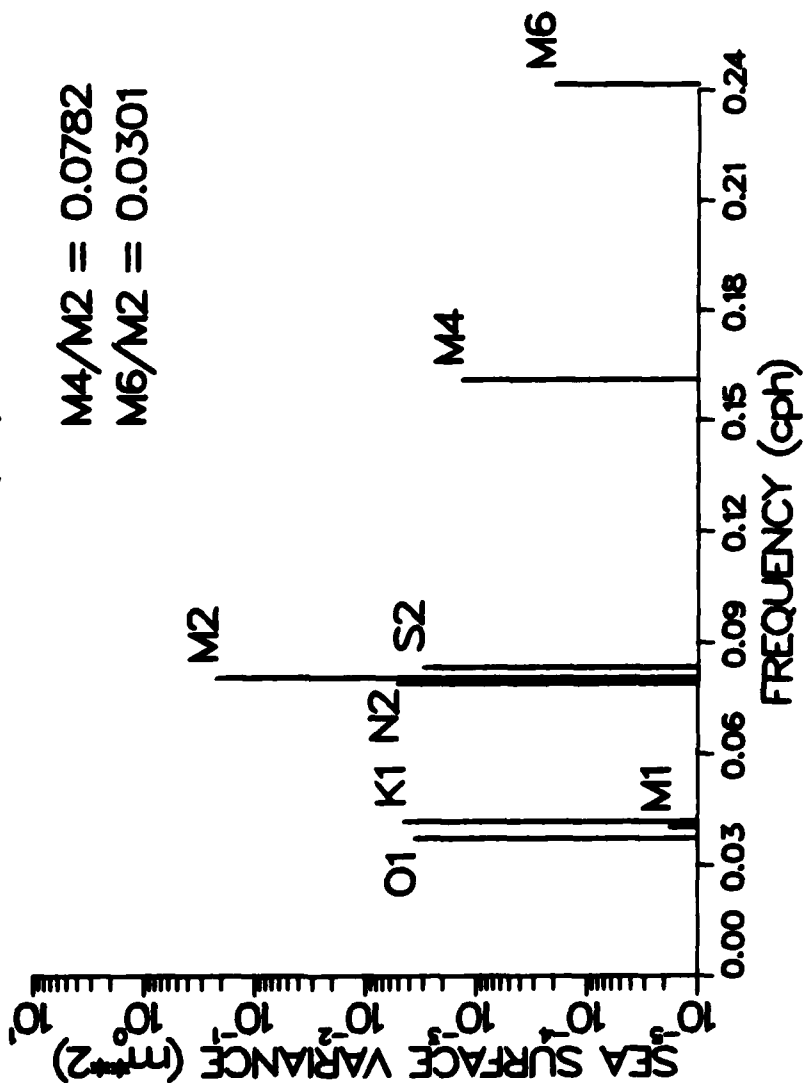
STATION: NAUSET HEIGHTS   LATITUDE: 41.80°N        LONGITUDE: 69.94°W

DATE:  30/9/82 - 29/10/82

| CONSTITUENT | AMPLITUDE (M) | $\zeta$ (deg.) | G (deg.) |
|---|---|---|---|
| $M_2$ | .616 | 304 | 114 |
| $S_2$ | .074 | 39 | 159 |
| $N_2$ | .103 | 162 | 91 |
| $K_1$ | .087 | 82 | 233 |
| $M_4$ | .068 | 174 | 155 |
| $O_1$ | .081 | 202 | 226 |
| $M_6$ | .014 | 255 | 46 |
| NU2 | .023 | 349 | 93 |
| MU2 | .015 | 206 | 69 |
| 2N2 | .016 | 19 | 66 |
| M1 | .006 | 322 | 229 |
| Q1 | .016 | 81 | 223 |
| P1 | .029 | 271 | 232 |
| L2 | .017 | 266 | 138 |
| K2 | .020 | 42 | 163 |

Recorded variance ($M^2$)     $2.44 \times 10^{-1}$

Residual variance ($M^2$)     $3.72 \times 10^{-2}$

NAUSET INLET TIDES
NAUSET HEIGHTS TIDE GAGE
30/9/82–10/29/82

M4/M2 = 0.1104
M6/M2 = 0.0227
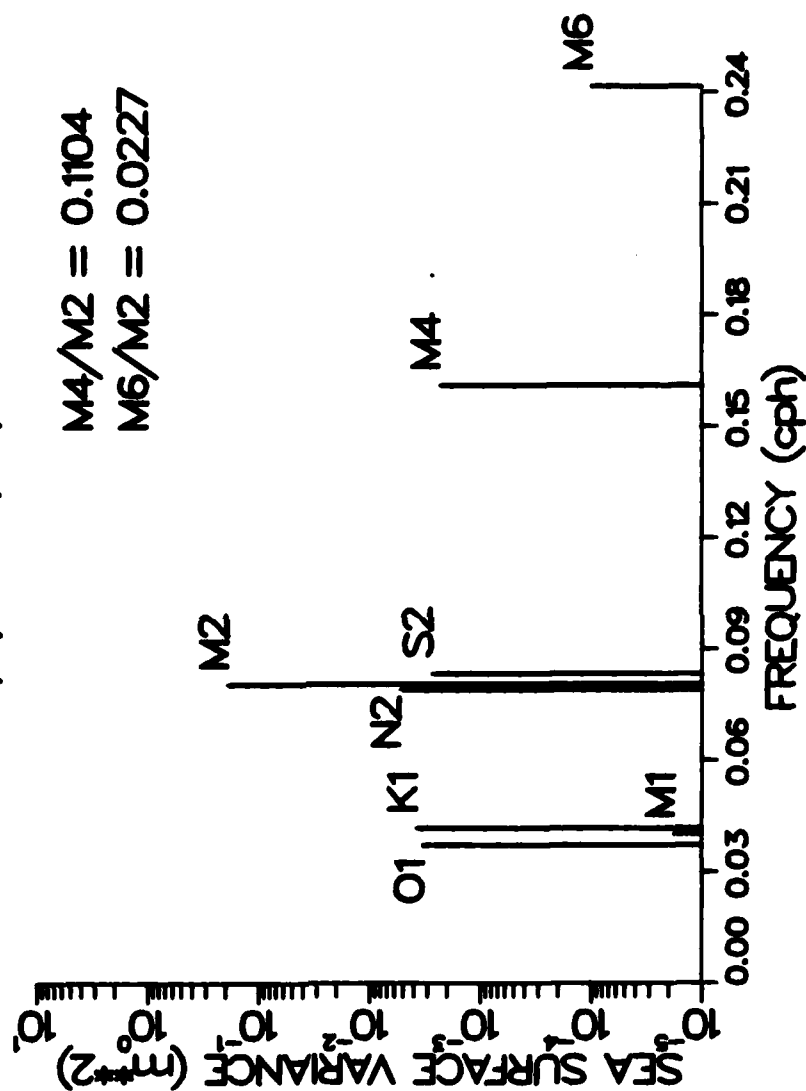
STATION: SNOW POINT     LATITUDE: 41.81°N     LONGITUDE: 69.96°W

DATE: 23/9/82 - 22/10/82

| CONSTITUENT | AMPLITUDE (M) | $\zeta$ (deg.) | G (deg.) |
|---|---|---|---|
| $M_2$ | .560 | 197 | 147 |
| $S_2$ | .062 | 101 | 188 |
| $N_2$ | .098 | 313 | 113 |
| $K_1$ | .090 | 126 | 253 |
| $M_4$ | .075 | 334 | 232 |
| $O_1$ | .083 | 55 | 241 |
| $M_6$ | .012 | 249 | 96 |
| NU2 | .021 | 165 | 128 |
| MU2 | .013 | 292 | 106 |
| 2N2 | .015 | 93 | 103 |
| M1 | .006 | 272 | 247 |
| Q1 | .016 | 199 | 235 |
| P1 | .030 | 300 | 252 |
| L2 | .016 | 250 | 169 |
| K2 | .017 | 118 | 191 |

     Recorded variance ($M^2$)     $2.09 \times 10^{-1}$

     Residual variance ($M^2$)     $3.53 \times 10^{-2}$

NAUSET INLET TIDES
SNOW POINT TIDE GAGE
23/9/82–22/10/82

M4/M2 = 0.1339
M6/M2 = 0.0214

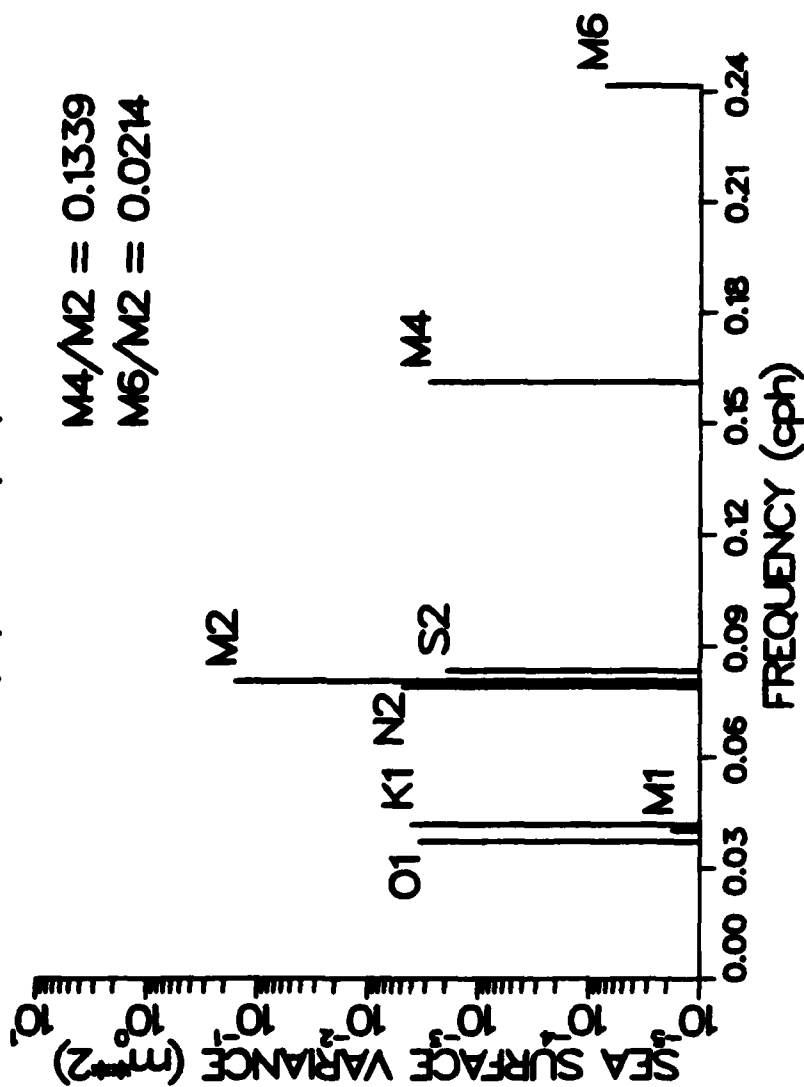STATION: SNOW POINT         LATITUDE: 41.81°N         LONGITUDE: 69.96°W

DATE: 25/8/82 - 23/9/82

| CONSTITUENT | AMPLITUDE (M) | $\zeta$ (deg.) | G (deg.) |
|---|---|---|---|
| $M_2$ | .534 | 240 | 148 |
| $S_2$ | .072 | 123 | 180 |
| $N_2$ | .091 | 322 | 100 |
| $K_1$ | .085 | 173 | 256 |
| $M_4$ | .074 | 57 | 231 |
| $O_1$ | .091 | 49 | 237 |
| $M_6$ | .012 | 31 | 112 |
| NU2 | .020 | 243 | 133 |
| MU2 | .013 | 356 | 115 |
| 2N2 | .014 | 106 | 113 |
| M1 | .006 | 300 | 247 |
| Q1 | .018 | 170 | 228 |
| P1 | .028 | 290 | 255 |
| L2 | .015 | 309 | 165 |
| K2 | .020 | 197 | 183 |

Recorded variance ($M^2$)      $1.71 \times 10^{-1}$

Residual variance ($M^2$)      $9.02 \times 10^{-3}$

NAUSET INLET TIDES
SNOW POINT TIDE GAGE
25/8/82–23/9/82

M4/M2 = 0.1386
M6/M2 = 0.0225
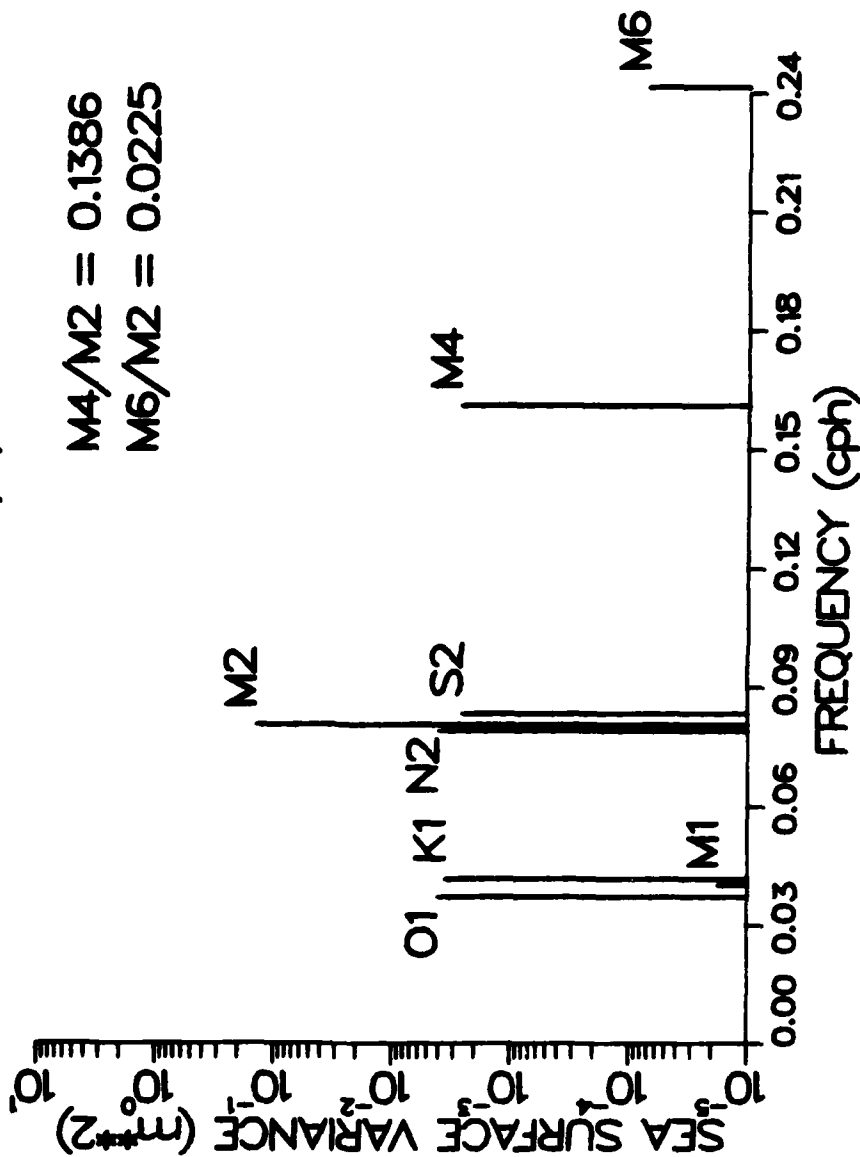
STATION: GOOSE HUMMOCK     LATITUDE: 41.80°N        LONGITUDE: 69.99°W

DATE: 22/7/82 - 20/8/82

| CONSTITUENT | AMPLITUDE (M) | $\zeta$ (deg.) | G (deg.) |
|---|---|---|---|
| $M_2$ | .521 | 115 | 152 |
| $S_2$ | .064 | 119 | 197 |
| $N_2$ | .115 | 113 | 103 |
| $K_1$ | .083 | 190 | 250 |
| $M_4$ | .116 | 168 | 241 |
| $O_1$ | .094 | 262 | 242 |
| $M_6$ | .017 | 343 | 234 |
| NU2 | .020 | 88 | 131 |
| MU2 | .013 | 110 | 106 |
| 2N2 | .014 | 160 | 103 |
| M1 | .007 | 242 | 246 |
| Q1 | .018 | 304 | 238 |
| P1 | .028 | 240 | 249 |
| L2 | .015 | 276 | 176 |
| K2 | .017 | 151 | 201 |

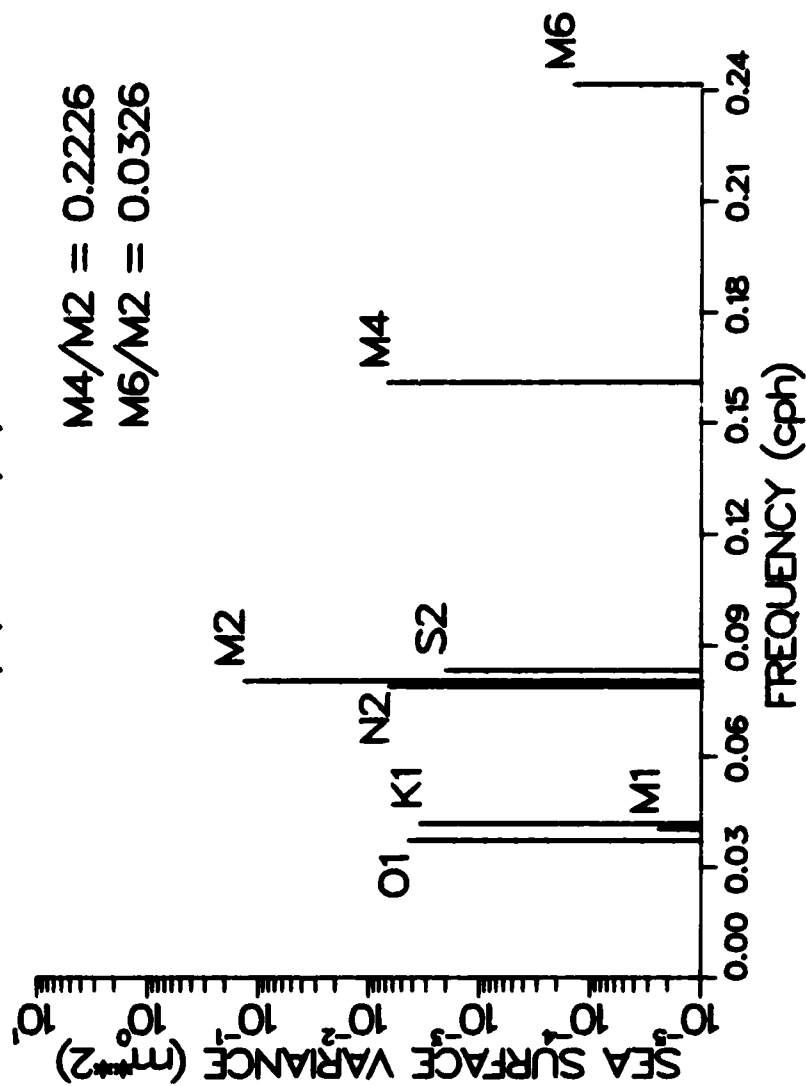Recorded variance ($M^2$)      $1.73 \times 10^{-1}$

Residual variance ($M^2$)      $8.94 \times 10^{-3}$

NAUSET INLET TIDES
GOOSE HUMMOCK TIDE GAGE
22/7/82-20/8/82

M4/M2 = 0.2226
M6/M2 = 0.0326

STATION: NORTH CHANNEL    LATITUDE: 41.82°N        LONGITUDE: 69.95°W

DATE: 13/9/81 - 11/10/81

| CONSTITUENT | AMPLITUDE (M) | $\zeta$ (deg.) | G (deg.) |
|---|---|---|---|
| $M_2$ | .450 | 6 | 145 |
| $S_2$ | .074 | 48 | 183 |
| $N_2$ | .109 | 286 | 134 |
| $K_1$ | .066 | 116 | 258 |
| $M_4$ | .086 | 311 | 228 |
| $O_1$ | .073 | 235 | 236 |
| $M_6$ | .003 | 229 | 286 |
| NU2 | .017 | 52 | 127 |
| MU2 | .011 | 322 | 107 |
| 2N2 | .012 | 180 | 104 |
| M1 | .005 | 58 | 247 |
| Q1 | .014 | 156 | 226 |
| P1 | .022 | 271 | 256 |
| L2 | .013 | 287 | 165 |
| K2 | .020 | 82 | 186 |

Recorded variance ($M^2$)     $1.35 \times 10^{-1}$

Residual variance ($M^2$)     $1.07 \times 10^{-2}$

NAUSET INLET TIDES
NORTH CHANNEL TIDE GAGE
13/9/81–11/10/81

M4/M2 = 0.1911
M6/M2 = 0.0067
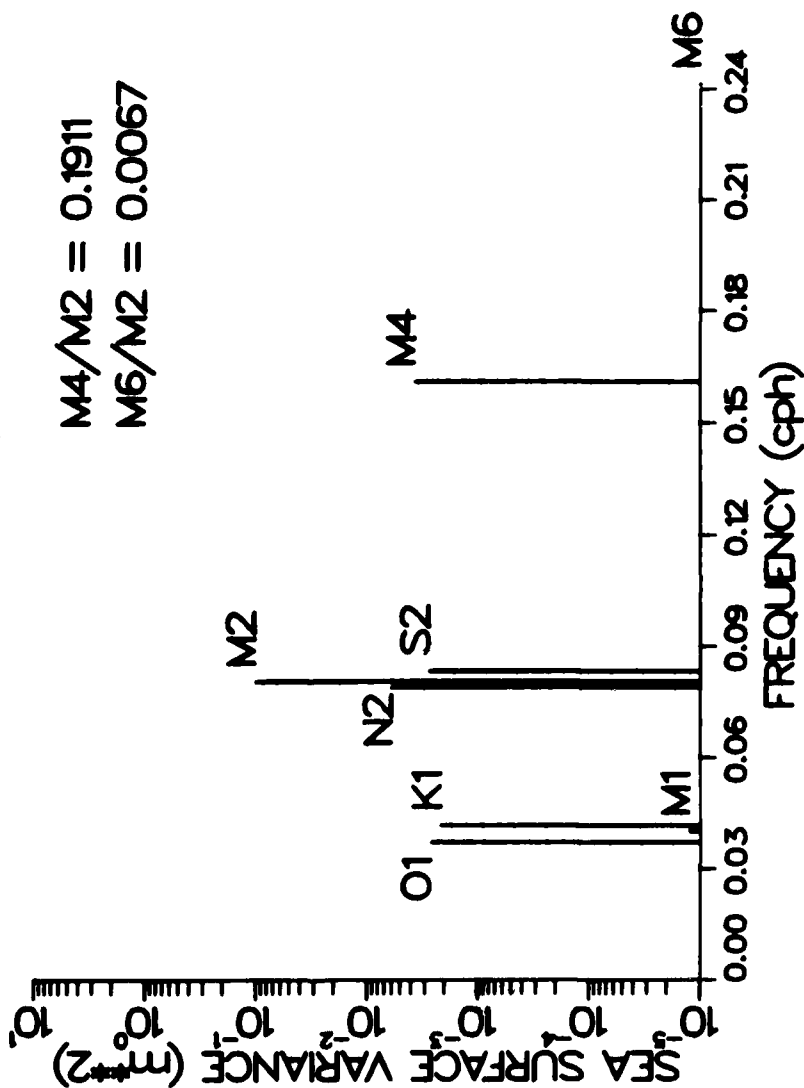
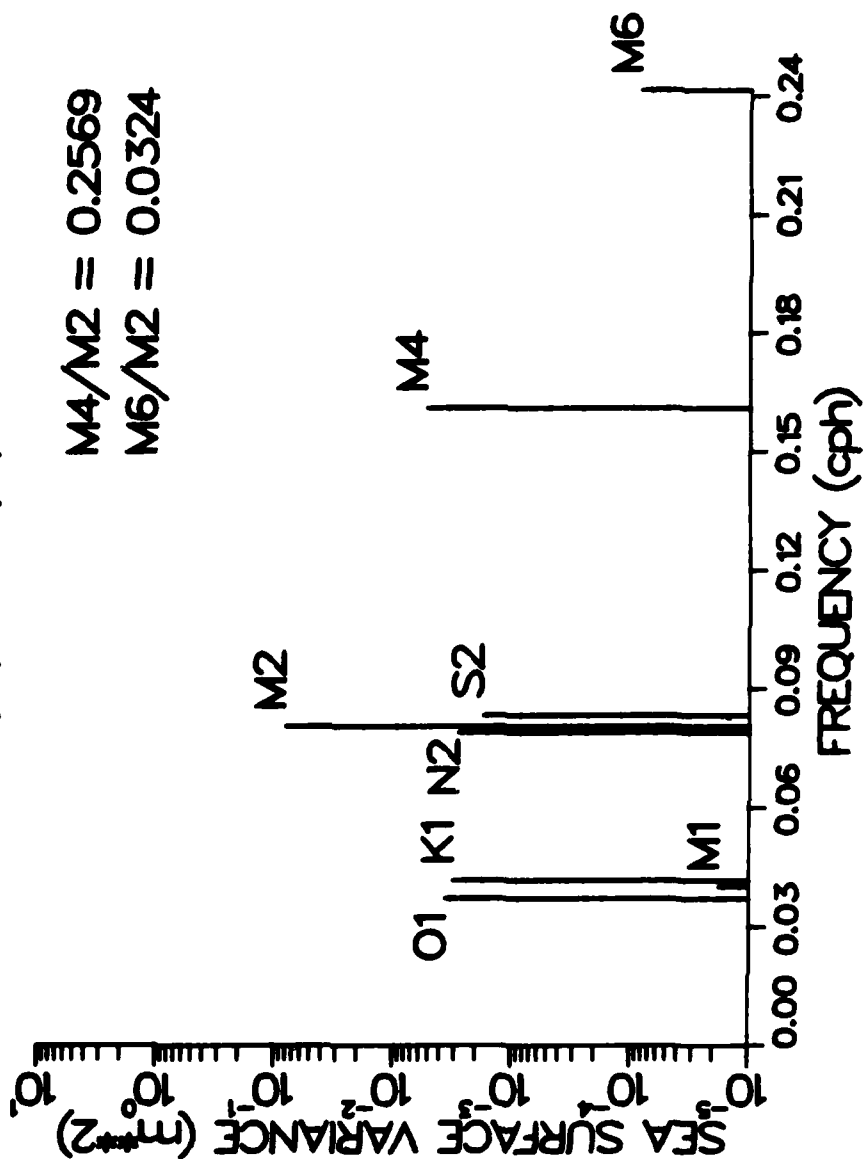STATION: NAUSET BAY     LATITUDE: 41.83°N     LONGITUDE: 69.96°W

DATE: 25/8/82 - 23/9/82

| CONSTITUENT | AMPLITUDE (M) | $\zeta$ (deg.) | G (deg.) |
|---|---|---|---|
| $M_2$ | .401 | 267 | 174 |
| $S_2$ | .059 | 143 | 200 |
| $N_2$ | .075 | 345 | 123 |
| $K_1$ | .079 | 187 | 270 |
| $M_4$ | .103 | 112 | 286 |
| $O_1$ | .085 | 64 | 252 |
| $M_6$ | .013 | 333 | 55 |
| NU2 | .015 | 272 | 162 |
| MU2 | .010 | 28 | 148 |
| 2N2 | .010 | 139 | 146 |
| M1 | .006 | 314 | 261 |
| Q1 | .016 | 184 | 243 |
| P1 | .026 | 304 | 269 |
| L2 | .011 | 332 | 188 |
| K2 | .016 | 216 | 202 |

Recorded variance ($M^2$)     $1.07 \times 10^{-1}$

Residual variance ($M^2$)     $8.87 \times 10^{-3}$

NAUSET INLET TIDES
NAUSET BAY TIDE GAGE
25/8/82–23/9/82

M4/M2 = 0.2569
M6/M2 = 0.0324

50272-101

| REPORT DOCUMENTATION PAGE | 1. REPORT NO. WHOI-83-20 | 2. | 3. Recipient's Accession No AD-A131388 |
|---|---|---|---|
| 4. Title and Subtitle **SEDIMENT TRANSPORT IN A TIDAL INLET** | | | 5. Report Date June 1983 |
| | | | 6. |
| 7. Author(s) David G. Aubrey and Paul E. Speer | | | 8. Performing Organization Rept. No WHOI-83-20 |
| 9. Performing Organization Name and Address Woods Hole Oceanographic Institution Woods Hole, Massachusetts 02543 | | | 10. Project/Task/Work Unit No. |
| | | | 11. Contract(C) or Grant(G) No. (C) DAAG 29-81-K-0004 NA79AA-D-00102 (G) NA80AA-D-00077 |
| 12. Sponsoring Organization Name and Address U.S. Army Research Office and Department of Commerce, NOAA, Office of Sea Grant | | | 13. Type of Report & Period Covered TECHNICAL 15/10/80 - 14-10-82 |
| | | | 14. |

15. Supplementary Notes

The views, opinions, and/or findings contained in this report are those of the (author(s) and should not be construed as an official Department of the Army position, policy, or decision, unless so designated by other documentation.

16. Abstract (Limit: 200 words)

Various aspects of sediment transport in and around natural, unstructured tidal inlets were investigated over the two year period of study. Concentrating on two tidal inlets (Nauset Inlet and Popponesset Inlet, Cape Cod, MA), and combining detailed field observations with numerical model studies of tidal flows in inlet/estuarine environments, several aspects of tidal inlet behavior have been clarified. In addition, field work has resulted in a number of technical publications of general utility to a wide spectrum of coastal research interest. Primary scientific items addressed in this study include: 1) diagnostic numerical model of generation and propagation of tidal non-liniarities in shallow estuarine channels; 2) effects of flow curvature on tidal inlet sediment transport; 3) definition of mechanisms by which tidal inlets migrate in a direction opposite to the net littoral drift direction; 4) hypothesis of a mechanism for rapid barrier spit growth in locations with low rates of littoral transport; 5) clarification of long-term patterns of sea-level rise in the United States to assess its role in tidal inlet/esturarine evolution; 6) historical descriptions of massive inlet migration at two study inlets as supporting evidence for the inlet modeling studies. Technical information generated by the study includes a description of a low-cost, reliable method to join nearshore electrical cables; description and intercomparison of instrumentation and analysis routines for estimating directional spectral parameters from wave gage data; and development of a field system and laboratory analysis package for preparing accurate bathymetric charts in shallow, nearshore regions, using microwave navigation and precision echo-sounding.

17. Document Analysis   a. Descriptors

1. Tidal Inlets; sediment transport

2. Shallow water tides

3. Barrier beaches

b. Identifiers/Open-Ended Terms

c. COSATI Field/Group

| 18. Availability Statement | 19. Security Class (This Report) Unclassified | 21. No. of Pages 110 |
|---|---|---|
| DISTRIBUTION STATEMENT A Approved for public release; Distribution Unlimited | 20. Security Class (This Page) | 22. Price |

(See ANSI–Z39.18)

OPTIONAL FORM 272 (4-77)
(Formerly NTIS-35)
Department of Commerce

END

FILMED

9-83

DTIC